Bijections for Baxter Families and Related Objects

Stefan Felsner*
Institut für Mathematik,
Technische Universität Berlin.
felsner@math.tu-berlin.de

Éric Fusy
Laboratoire d'Informatique (LIX)
École Polytechnique.
fusy@lix.polytechnique.fr

Marc Noy
Departament de Matemàtica Aplicada II
Universitat Politècnica de Catalunya.
marc.noy@upc.edu

David Orden†
Departamento de Matemáticas
Universidad de Alcalá
david.orden@uah.es

Abstract

The Baxter number B_n can be written as $B_n = \sum_0^n \Theta_{k,n-k-1}$ with

$$\Theta_{k,\ell} = \frac{2}{(k+1)^2\,(k+2)}\binom{k+\ell}{k}\binom{k+\ell+1}{k}\binom{k+\ell+2}{k}.$$

These numbers have first appeared in the enumeration of so-called Baxter permutations; B_n is the number of Baxter permutations of size n, and $\Theta_{k,\ell}$ is the number of Baxter permutations with k descents and ℓ rises. With a series of bijections we identify several families of combinatorial objects counted by the numbers $\Theta_{k,\ell}$. Appart from Baxter permutations, these include plane bipolar orientations with $k+2$ vertices and $\ell+2$ faces, 2-orientations of planar quadrangulations with $k+2$ white and $\ell+2$ black vertices, certain pairs of binary trees with $k+1$ left and $\ell+1$ right leaves, and a family of triples of non-intersecting lattice paths. This last family allows us to determine the value of $\Theta_{k,\ell}$ as an application of the lemma of Gessel and Viennot. The approach also allows us to count certain other subfamilies, e.g., alternating Baxter permutations, objects with symmetries and, via a bijection with a class of plan bipolar orientations also Schnyder woods of triangulations, which are known to be in bijection with 3-orientations.

Mathematics Subject Classifications (2000). 05A15, 05A16, 05C10, 05C78

1 Introduction

This paper deals with combinatorial families enumerated by either the Baxter numbers or the summands $\Theta_{k,\ell}$ of the usual expression of Baxter numbers. Many of the enumeration results have been known, even with bijective proofs. Our contribution to these cases lies in the integration into a larger context and in simplified bijections. We use specializations of the general bijections to count certain subfamilies, e.g., alternating Baxter permutations, objects with symmetries and Schnyder woods, i.e., 3-orientations of triangulations.

*Partially supported by DFG grant FE-340/7-1
†Research partially supported by grants MTM2005-08618-C02-02 and S-0505/DPI/0235-02.

This introduction will not include definitions of the objects we deal with, nor bibliographic citations, which are gathered in notes throughout the article. Therefore, we restrict it to a kind of commented table of contents.

2 Separating Decompositions and Book Embeddings

In the context of this paper a *quadrangulation* is a plane graph $Q = (V \cup \{s,t\}, E)$ with only quadrangular faces. More precisely, Q is a maximal bipartite plane graph, with $n+2$ vertices, prescribed color classes black and white and two distinguished black vertices s and t on the outer face. Note that Q has n faces and $2n$ edges. *quadrangulation*

Definition 2.1. An orientation of the edges of Q is a *2-orientation* if every vertex, except the two special vertices s and t, has outdegree two. From easy arguments on double-counting the edges of Q, s and t are sinks in every 2-orientation. *2-orientation*

Definition 2.2. An orientation and coloring of the edges of Q with colors red and blue is a *separating decomposition* if: *separating decomposition*

(1) All edges incident to s are red and all edges incident to t are blue.

(2) Every vertex $v \neq s,t$ is incident to an interval of red edges and an interval of blue edges. If v is white, then, in clockwise order, the first edge in the interval of a color is outgoing and all the other edges of the interval are incoming. If v is white the outgoing edge is the clockwise last in its color. (c.f. Figure 1)

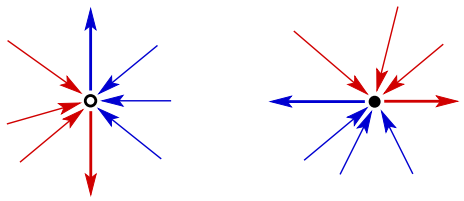

Figure 1: Edge orientations and colors at white and black vertices.

Theorem 2.1. *Let $Q = (V \cup \{s,t\}, E)$ be a plane quadrangulation. Separating decompositions and 2-orientations of Q are in bijection.*

Proof. A separating decomposition clearly yields a 2-orientation, just forget the coloring. For the converse, let (v,w) be an oriented edge, and define the *left-right path* of the edge as the directed path starting with (v,w) and taking a left-turn in black vertices and a right-turn in white vertices. *left-right path*

Claim A. Every left-right path ends in one of the special vertices.

Proof of the claim. Suppose a left-right path closes a cycle C. The length of C is an even number $2k$. Let r be the number of vertices interior to C. Consider the inner quadrangulation of C. By Euler's formula it has $2r + 3k - 2$ edges. However, when we sum up the outdegrees of the vertices we find that k vertices on C contribute 1 while all other vertices contribute 2 which gives a total of $2r + 3k$, contradiction. △

Now, let the special vertex where a left-right path ends determine the color of all the edges along the path.

Claim B. The two left-right paths starting at a vertex do not meet again.

Proof of the claim. Suppose that the two paths emanating from v meet again at w. The two paths form a cycle C of even length $2k$ with r inner vertices. By Euler's formula the

inner quadrangulation of C has $2r + 3k - 2$ edges. From the left-right rule we know that one neighbor of v on C has an edge pointing into the interior of C, from which it follows that there are at least $k - 1$ edges pointing from C into its interior. Hence, there are at least $2r + 3k - 1$ edges, contradiction. △

Consequently, the two outgoing edges of a vertex v receive different colors. It follows that the orientation and coloring of edges is a separating decomposition. □

From the proof we obtain an additional property of a separating decomposition:

(3) *The red edges form a directed tree rooted in s and the blue edges form a tree rooted in t.*

Note.

De Fraysseix and Ossona de Mendez [14] defined a separating decomposition via properties (1), (2) and (3), i.e., they included the tree-property into the definition. They also proved Claim A and B and concluded Theorem 2.1. In [14] it is also shown that every quadrangulation admits a 2-orientation.

An embedding of a plane graph is called a *2-book embedding* if the vertices are arranged on a single line so that all edges are either below or above the line. As we show next, a separating decomposition S easily yields a 2-book embedding of the underlying quadrangulation Q.

Observe that each inner face of Q has exactly two bicolored angles, i.e., angles where edges of different color meet; this follows from the rules given in Definition 2.2. Define the *equatorial line* of S as the union of all diagonals connecting bicolored angles of an inner face. The definition of a separating decomposition implies that each inner vertex of Q has degree two in the equatorial line, while s and t have degree zero and the other two outer vertices have degree one. This implies that the equatorial line consists of an edge-disjoint union of a path and possibly a collection of cycles.

equatorial line

Lemma 2.1. *Given a quadrangulation Q endowed with a separating decomposition S, the equatorial line of S consists of a single path that traverses every inner vertex and every inner face of Q exactly once.*

Proof. Assume that the equatorial line has a cycle C. Consider a plane drawing of $Q \cup C$. The cycle C splits the drawing into an inner and an outer part, both special vertices s and t being in the outer part. The red edges of all vertices of C emanate to one side of C while the blue edges go to the other side. Therefore, it is impossible to have a monochromatic path from a vertex $v \in C$ to both special vertices. With property (3) of separating decompositions, it thus follows that there are no cycles, i.e., the equatorial line is a single path.

The equatorial line L has the two outer non-special vertices of Q as extremities. It has degree 2 for each inner vertex, hence it traverses each inner vertex once. In addition, L separates the blue and the red edges, hence it must pass through the interior of each inner face at least once. Since the n non-special vertices of Q delimit $n - 1$ intervals on L and since Q has $n - 1$ inner faces, L can only pass through each inner face exactly once. □

To produce a 2-book embedding, extend the equatorial line in the outer face so that it visits also the two special vertices; then stretch the equatorial line as a straight horizontal line that has s as its leftmost vertex and t as its rightmost vertex, see Figure 2. Observe that one page gathers the blue edges, the other page gathers the red edges, and the spine for the two pages is the equatorial line.

The equatorial line will be useful again for proving a Hamiltonicity result in Section 5.2.

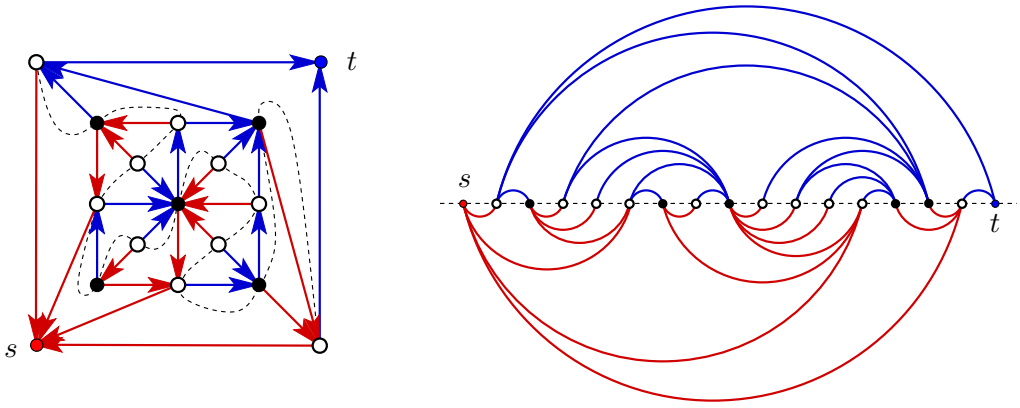

Figure 2: A quadrangulation Q with a separating decomposition S, and the 2-book embedding induced by the equatorial line of S.

Definition 2.3. An *alternating layout* of a tree T with $n+1$ vertices is a non-crossing drawing of T such that its vertices are mapped to different points on the non-negative x-axis and all edges are embedded in the halfplane above the x-axis (or all below). Moreover, for every vertex v it holds that all its neighbors are on one side, either they are all left of v or all right of v. In these cases we call the vertex v respectively a *right* or a *left vertex* of the alternating layout. A tree with an alternating layout is an *alternating tree*.

alternating layout

right
left vertex
alternating tree

As one can check in the example of Figure 2, the red and the blue trees are both alternating. Indeed, by the rules given in Definition 2.2, white vertices are right in the red tree and left in the blue tree while black vertices are left in red and right in blue. We summarize:

Proposition 2.1. The 2-book embedding induced by a separating decomposition yields simultaneous alternating layouts of the two trees such that each white vertex is left in the blue tree and right in the red tree, while each black vertex is right in the blue tree and left in the red tree.

Note.

A proof of Proposition 2.1 was given by Felsner, Huemer, Kappes and Orden [20]. These authors study what they call *strong binary labelings of the angles of a quadrangulation*. They show that these labelings are in bijection with 2-orientations and separating decompositions. In this context they find the 2-book embedding; their method consists in ranking each vertex v on the spine of the 2-book embedding according to the number of faces in a specific region $R(v)$. The original source for a 2-book embedding of a quadrangulation is [15], by de Fraysseix, Ossona de Mendez and Pach. General planar graphs may require as many as 4 pages for a book embedding, Yannakakis [43].

Alternating trees in our sense were studied by Rote, Streinu and Santos [36] as *non-crossing alternating trees*. There it is pointed out that the name *alternating tree* is sometimes used to denote a tree with a numbering such that every vertex is a local extremum, e.g., [40, Exercise 5.41]. Non-crossing alternating trees were studied by Gelfand et al. [26] under the name of *standard trees*; there it is shown that these trees are a Catalan family. In [36] connections with rigidity theory and the geometry of the associahedron are established.

Consider alternating layouts of rooted ordered trees with the property that the root is extreme, i.e., the root is either the leftmost or the rightmost of the vertices. In this setting an alternating layout is completely determined by the placement of the root (left/right) and the choice of a halfplane for the edges (above/below). We denote the four choices with symbols, e.g., $\swarrow$ denotes that the root is left and the halfplane below; the symbols $\nwarrow$, $\nearrow$ and $\searrow$ represent the other three possibilities.

The unique $\swarrow$-alternating layout of T, is obtained by starting at the root and walking clockwise around T, thereby numbering the vertices with consecutive integers according to the following rules: The root is numbered 0 and all vertices in the color class of the root receive a number at the first visit while the vertices in the other color class receive a number at the last visit. Figure 3 shows an example. Rules for the other types of alternating layouts are:

$\nwarrow$-layout: walk counterclockwise, root class at first visit, other at last visit.

$\nearrow$-layout: walk counterclockwise, root class at last visit, other at first visit.

$\searrow$-layout: walk clockwise, root class at last visit, other at first visit.

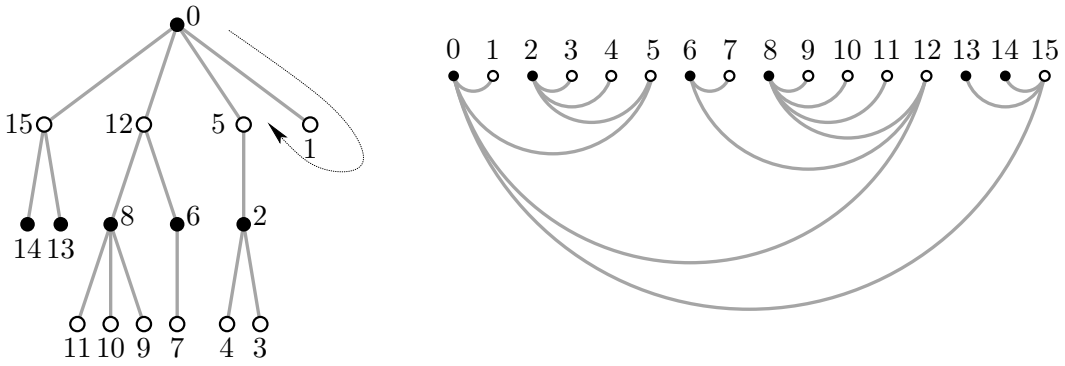

Figure 3: A tree, the numbering and the $\swarrow$-alternating layout.

The $\swarrow$-*fingerprint*, denoted $\alpha_{\swarrow}(T)$, of a rooted ordered tree T, is a $0,1$ string which has a 1 at position i, i.e., $\alpha_i = 1$, if the ith vertex in the $\swarrow$-alternating layout of T is a left vertex, otherwise, if the vertex is a right vertex $\alpha_i = 0$. The $\swarrow$-fingerprint of the tree T from Figure 3 is $\alpha_{\swarrow}(T) = 1010001010000110$. Other types of fingerprints are defined by the same rule. For example the $\nearrow$-fingerprint of the tree in Figure 3 is $\alpha_{\nearrow}(T) = 1001111010111010$. With the numbering from Figure 3 this corresponds to the vertex order $0, 15, 14, 13, 12, 11, 10, 9, 8, 7, 6, 5, 4, 3, 2, 1$. *$\swarrow$-fingerprint*

The first vertex is always a left vertex and the last a right vertex, therefore, a fingerprint has always a 1 as first entry and a 0 as last entry. A *reduced fingerprint* $\hat{\alpha}_{\swarrow}(T)$, of a tree T is obtained by omitting the first and the last entry from the corresponding fingerprint. For a $0,1$ string s we define $\rho(s)$ to be the reverse string and $\overline{s}$ to be the complemented string. Example: if $s = 11010$, then $\rho(s) = 01011$, $\overline{s} = 00101$, and $\overline{\rho(s)} = \rho(\overline{s}) = 10100$. *reduced fingerprint*

Lemma 2.2. *For every tree T we have $\alpha_{\swarrow}(T) = \overline{\rho(\alpha_{\nearrow}(T))}$ (and $\alpha_{\nwarrow}(T) = \overline{\rho(\alpha_{\searrow}(T))}$).*

Proof. Take the $\nearrow$-alternating layout of T and rotate it by 180°. This results in the $\swarrow$-alternating layout. Observe what happens to the fingerprint. □

Definition 2.4. A pair (S,T) of rooted, oriented trees whose fingerprints satisfy $\hat{\alpha}_{\swarrow}(S) = \overline{\hat{\alpha}_{\nearrow}(T)}$, or equivalently $\hat{\alpha}_{\nearrow}(S) = \rho(\hat{\alpha}_{\nearrow}(T))$, is called a *twin-alternating pair of trees.*

twin-alternating pair of trees

Theorem 2.2. *There is a bijection between twin-alternating pairs of trees (S,T) on n vertices and 2-orientations of quadrangulations on $n+2$ vertices.*

Proof. (The bijection is illustrated with an example in Figure 4.) Augment both rooted ordered trees S and T by a new vertex which is made the rightmost child of the root. Let S^+ and T^+ be the augmented trees. Note that $\hat{\alpha}_{\swarrow}(S^+) = 0 + \hat{\alpha}_{\swarrow}(S)$ and $\hat{\alpha}_{\nearrow}(T^+) = \hat{\alpha}_{\nearrow}(T) + 1$. Since the first entry of a non-reduced fingerprint is always 1 and the last one is always 0 it follows that $\alpha_{\swarrow}(S^+) + 0 = \overline{1 + \alpha_{\nearrow}(T^+)}$.

Consider the $\swarrow$-alternating layout of S^+ and move the vertices in this layout to the integers $0, .., n$. Similarly, the $\nearrow$-alternating layout of T^+ is placed such that the vertices correspond to the integers $1, .., n+1$. At every integer $0 < i < n+1$ a vertex of S^+ and a vertex of T^+ meet. We identify them. As a consequence of the complemented fitting of the fingerprints, every non-special vertex is a left vertex in one of the layouts and a right vertex in the other. This has strong consequences:

- A pair uv can be an edge in at most one of S and T, otherwise u would have a neighbor on its right in both S and T, a contradiction.
- There is no triangle with edges from $S \cup T$. Suppose u, v, w would be such a triangle. Two edges must be from the same tree, say from S. These cannot be the two edges incident to the middle vertex v. If they are incident to w the vertex u has neighbors to its right in both trees, contradiction.

Hence, the graph with edges $S^+ \cup T^+$ is simple, triangle-free and non-crossing. Since it has $n+2$ vertices and $2n$ edges, it must be a quadrangulation. The 2-orientation is obtained by orienting both trees towards the root.

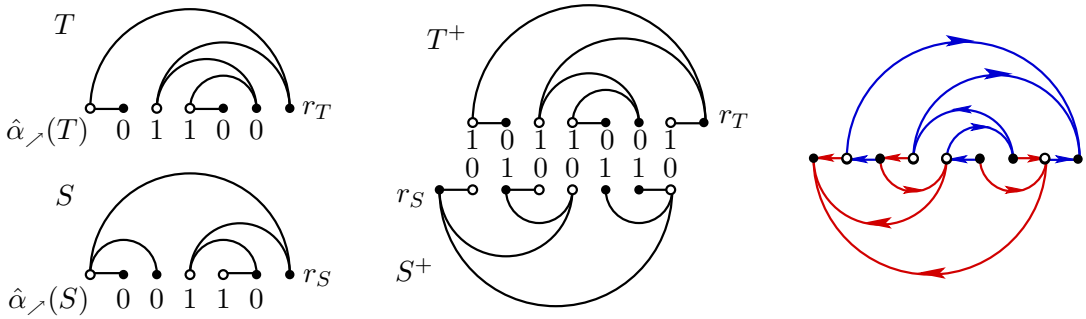

Figure 4: A twin-alternating pair of trees (S,T). The $\nearrow$-alternating layout of T^+ and the $\swarrow$-alternating layout of S^+ properly adjusted. The induced 2-orientation of a quadrangulation.

The converse direction, from the 2-orientation of a quadrangulation on $n+2$ vertices to trees (S,T) with appropriate fingerprints was already indicated. To recapitulate: A 2-orientation of Q yields a separating decomposition (Theorem 2.1). In particular the edges are decomposed into two trees, the red tree S^+ and the blue tree T^+. The corresponding 2-book embedding (Proposition 2.1) induces a simultaneous alternating layout of the two trees with the property that every non-special vertex is left in one of the trees and right in the other (Proposition 2.1), i.e., $\alpha_{\swarrow}(S^+) + 0 = \overline{1 + \alpha_{\nearrow}(T^+)}$. Trees S and T are obtained by deleting the left child of the root in S^+ and the right child of the root in T^+; they are both leaves and

correspond to the two non-special outer vertices of Q. Trees S and T satisfy $\hat{\alpha}_{\swarrow}(S) = \overline{\hat{\alpha}_{\nearrow}(T)}$, i.e., (S, T) is a twin-alternating pair of trees. □

3 Alternating Trees and other Catalan Families

A *full binary tree* is a rooted ordered tree such that each inner vertex has exactly two children. The *fingerprint* of a full binary tree T is a $0,1$ string which has a 1 at position i if the ith leaf of T is a left child, otherwise, if the leaf is a right child the entry is 0. In Figure 5 the tree T on the right side has $\alpha(T) = 1011101011110010$. The *reduced fingerprint* $\hat{\alpha}(T)$ is obtained by omitting the first and the last entry from $\alpha(T)$. Note that the first entry is always 1 and the last one is always 0.

full binary tree
fingerprint
reduced fingerprint

Proposition 3.1. There is a bijection $T \to T^\lambda$ which takes an alternating tree T with n vertices to a full binary tree T^λ with n leaves such that $\hat{\alpha}_{\nearrow}(T) = \hat{\alpha}(T^\lambda)$.

Proof. The bijection makes a correspondence between edges of the alternating tree and inner vertices of the full binary tree, see Figure 5. Embed T with vertices on integers from 0 to n. With an edge i, j of T associate an inner vertex x_{ij} for T^λ which is to be placed at $(\frac{i+j}{2}, \frac{j-i}{2})$. Draw line segments from the vertex $(i, 0)$ to x_{ij} and from $(j, 0)$ to x_{ij}. Doing this for every edge of T results in a drawing of the binary tree T^λ.

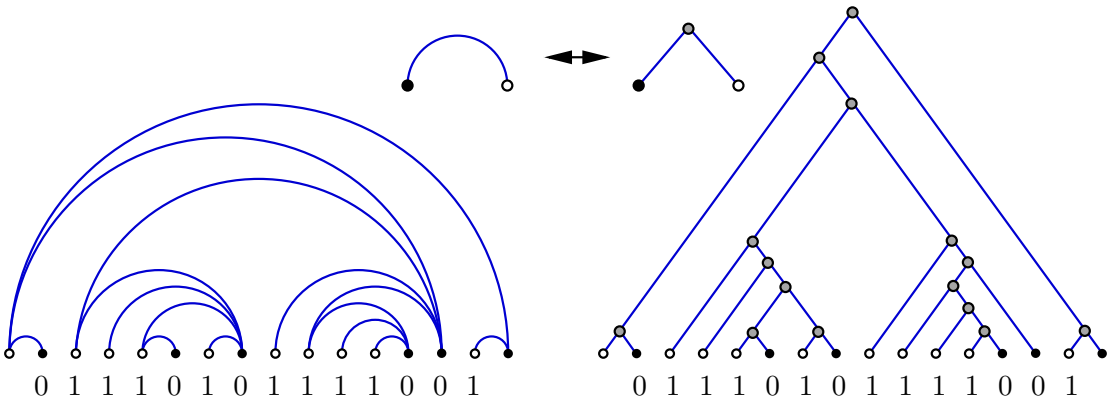

Figure 5: An $\nearrow$- alternating tree T and the full binary tree T^λ.

The converse is even simpler. Every inner node x of the binary tree gives rise to an edge connecting the leftmost leaf below x to the rightmost leaf below x. □

Note.

Full binary trees with $n+1$ leaves are counted by the *Catalan number* $C_n = \frac{1}{n+1}\binom{2n}{n}$. Catalan numbers are found in The On-Line Encyclopedia of Integer Sequences [39] as sequence A000108. From Proposition 3.1 it follows that alternating trees with $n+1$ vertices are another Catalan family, which in [26] was proved constructing a bijection inductively. Stanley [40, Exercise 6.19] collected 66 Catalan families.

Catalan number

Although the subject is well-studied, we include a particular proof showing that full binary trees are a Catalan family. Actually, we prove a more refined count related to Narayana numbers. The proof will be used later in the context of Baxter numbers.

To start with, we associate another $0,1$ string with a full binary tree T. The *bodyprint* $\beta(T)$ of T is obtained from a visit to the inner vertices of T in-order. The ith entry of β is a 1, i.e., $\beta_i = 1$, if the ith inner vertex is a right-child or it is the root. If the vertex is a left-child, then $\beta_i = 0$. Note that if the tree T is drawn such that all leaves are on a horizontal line, then there is a one-to-one correspondence between inner vertices and the gaps between adjacent leaves (Gap between leaves v_i and $v_{i+1} \mapsto$ least common ancestor of v_i and v_{i+1}. Inner vertex $x \mapsto$ gap between rightmost leaf in left subtree below x and leftmost leaf in right subtree below x). This correspondence maps the left-to-right order of gaps between leaves to the in-order of inner vertices. Since the root contributes a 1 the last entry of the bodyprint of a tree is always 1. Therefore, it makes sense to define the *reduced bodyprint* $\hat{\beta}(T)$ as $\beta(T)$ minus the last entry. Figure 6 shows an example.

bodyprint

reduced bodyprint

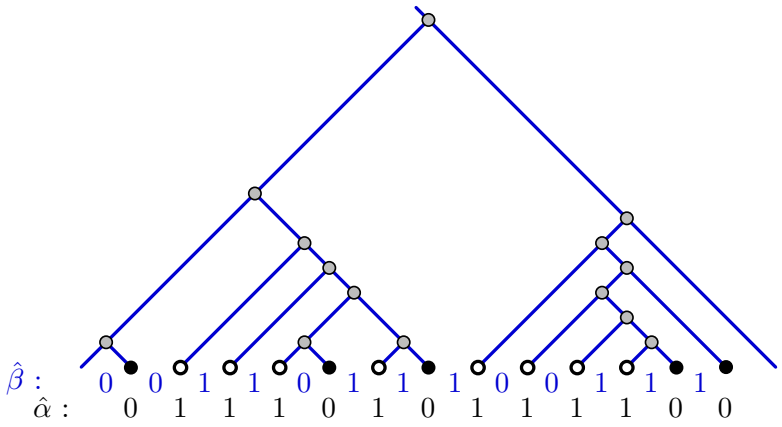

Figure 6: A full binary tree with reduced bodyprint $\hat{\beta}$ and reduced fingerprint $\hat{\alpha}$.

Lemma 3.1. *Let T be a full binary tree with with k left leaves and $n-k+1$ right leaves. The reduced fingerprint $\hat{\alpha}(T)$ and the reduced bodyprint $\hat{\beta}(T)$ both have length $n-1$. Moreover:*

$$(1) \quad \sum_{i=1}^{n-1} \hat{\alpha}_i = \sum_{i=1}^{n-1} \hat{\beta}_i = k-1 \qquad (2) \quad \sum_{i=1}^{j} \hat{\alpha}_i \geq \sum_{i=1}^{j} \hat{\beta}_i \quad \text{for all } j = 1, \ldots, n-1.$$

Proof. Consider a drawing of T where every edge has slope 1 or -1, as in Figure 6. The maximal segments of slope 1 in this drawing define a matching M between the k left leaves, i.e., 1-entries of $\alpha(T)$, and inner vertices which are right-childs including the root, i.e., 1-entries of $\beta(T)$. The left part of Figure 7 indicates the correspondence. The reduction $\hat{\alpha}$ (resp. $\hat{\beta}$) has exactly one 1-entry less than α (resp. β). This proves (1).

For (2) let $v_0, v_1, \ldots, v_n$ be the set of leaves in left-to-right order and let $x_1, \ldots, x_n$ be the in-order of inner vertices. Note that v_i determines α_i and x_i determines β_i. Let (v_i, x_j) be a pair from the matching M defined above, i.e., $\alpha_i = 1$ and $\beta_j = 1$. Since v_i is the leftmost leaf below x_j and the gap corresponding to x_j starts at the rightmost vertex v_{j-1} of the left subtree of x_j we find that $i \leq j-1$. This gives a matching between the 1-entries of α and the 1-entries of β with the property that the index of the 1-entry of α is always less that the index of the mate in β.

To conclude the inequality for the reduced strings we have to address another detail: The mate of the root in M is the leaf v_0, which is not represented in $\hat{\alpha}$, and there is a leaf whose mate in M is the last inner vertex x_n, which is not represented in $\hat{\beta}$. Consider the ordered

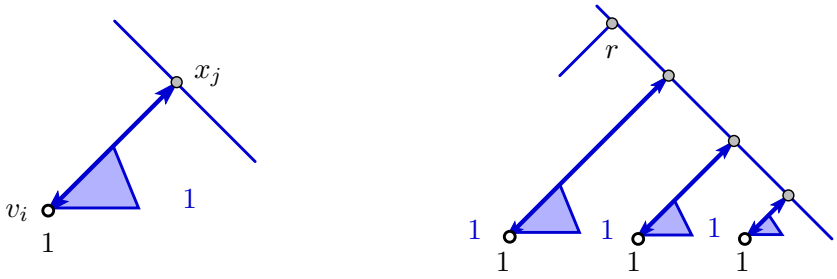

Figure 7: Illustrations for the proof of Lemma 3.1. The pair (v_i, x_j) is in M.

sequence $x_{j_0}, x_{j_1}, \ldots, x_{j_s}$ of all vertices on the rightmost branch of T, such that x_{j_0} is the root r and $x_{j_s} = x_n$. The right part of Figure 7 may help to see that in M we have the following pairs $(v_0, x_{j_0}), (v_{j_0}, x_{j_1}), \ldots (v_{j_{s-1}}, x_n)$; in particular $\alpha_0 = \alpha_{j_0} = \ldots = \alpha_{j_{s-1}} = 1$ and $\beta_{j_0} = \beta_{j_1} = \ldots = \beta_n = 1$. Hence we can define a matching M' which is as M except that v_0 and x_n remain unmatched and the pairs (v_{j_i}, x_{j_i}) with $0 \leq i \leq s-1$ are matched. This matching M' between the 1-entries of $\hat{\alpha}$ and the 1-entries of $\hat{\beta}$ has the property that the index of the 1-entry of $\hat{\alpha}$ is always at most the index of the mate in $\hat{\beta}$. This proves (2). □

Definition 3.1. With $\sigma \in \binom{k+\ell}{k}$ we denote that σ is a $0,1$ string of length $n = k + \ell$ with k entries 1 and ℓ entries 0, i.e., $\sum_{i=1}^{n} \sigma_i = k$. For $\sigma, \tau \in \binom{k+\ell}{k}$ we define $\tau \geq_{\mathsf{dom}} \sigma$, i.e., τ *dominates* σ, if $\sum_{i=1}^{j} \tau_i \geq \sum_{i=1}^{j} \sigma_i$ for all $j = 1, \ldots, n$. *dominates*

Theorem 3.1. *The mapping $T \leftrightarrow (\hat{\beta}, \hat{\alpha})$ is a bijection between full binary trees with $k+1$ left leaves and $\ell+1$ right leaves and pairs $(\hat{\beta}, \hat{\alpha})$ of $0,1$ strings in $\binom{k+\ell}{k}$ with $\hat{\alpha} \geq_{\mathsf{dom}} \hat{\beta}$.*

Proof. From Lemma 3.1 we know that reduced body- and fingerprint have the required properties. To show that the mapping $T \leftrightarrow (\hat{\beta}, \hat{\alpha})$ is a bijection we use induction.

First note that $\hat{\alpha} = 0^\ell 1^k$ implies $\hat{\beta} = \hat{\alpha}$, and that there are unique trees with these reduced finger- and bodyprints.

If $\hat{\alpha}$ has a different structure, then there is an i such that $\hat{\alpha}_{i-1}\hat{\alpha}_i = 10$. In a hypothetical tree T corresponding to $(\hat{\beta}, \hat{\alpha})$, the pair v_{i-1}, v_i is a left leaf followed by a right leaf. The leaves v_{i-1} and v_i are children of the inner vertex x_i, the value $\hat{\beta}_i = 1$ or $\hat{\beta}_i = 0$ depends on whether x_i is itself a left or a right child. Consider the tree T^* obtained by pruning the two leaves v_{i-1} and v_i. Note that if $\hat{\alpha}(T) = \hat{\alpha}'\, \hat{\alpha}_{i-1}\, \hat{\alpha}_i\, \hat{\alpha}''$ and $\hat{\beta}(T) = \hat{\beta}'\, \hat{\beta}_i\, \hat{\beta}''$, then $\hat{\beta}(T^*) = \hat{\beta}'\, \hat{\beta}''$ and $\hat{\alpha}(T^*) = \hat{\alpha}'\, \delta\, \hat{\alpha}''$ where $\delta = 1$ if $\hat{\beta}_i = 0$ and $\delta = 0$ if $\hat{\beta}_i = 1$.

Hence, we define $\hat{\alpha}^* = \hat{\alpha}'\, \delta\, \hat{\alpha}''$ and $\hat{\beta}^* = \hat{\beta}'\, \hat{\beta}''$. Depending on the value of $\delta = \overline{\hat{\beta}_i}$, this can be interpreted as either having removed the two entries $\hat{\beta}_i = 1$ and $\hat{\alpha}_{i-1} = 1$ or the two entries $\hat{\beta}_i = 0$ and $\hat{\alpha}_i = 0$ from $\hat{\alpha}$ and $\hat{\beta}$. It is easy to check that $\hat{\alpha}^* \geq_{\mathsf{dom}} \hat{\beta}^*$. By induction there is a unique tree T^* with n leaves such that $(\hat{\beta}(T^*), \hat{\alpha}(T^*)) = (\hat{\beta}^*, \hat{\alpha}^*)$. Making the ith leaf of T^* an inner vertex with two leaf children yields the unique tree T with $(\hat{\beta}(T), \hat{\alpha}(T)) = (\hat{\beta}, \hat{\alpha})$. □

There is a natural correspondence between $0,1$ strings $\sigma \in \binom{k+\ell}{k}$ and *upright lattice paths* P_σ from $(0,0)$ to (ℓ, k), which takes an entry 1 from σ to a step to the right, i.e., the addition of $(1,0)$ to the current position, and an entry 0 from σ to a step upwards, i.e., the addition of $(0,1)$ to the current position. *upright lattice paths*

This correspondence is the heart of a correspondence between pairs $(\sigma, \tau) \in \binom{k+\ell}{k}$ with $\tau \geq_{\mathsf{dom}} \sigma$, and pairs (P_σ, P_τ) of non-intersecting lattice paths, where P_σ is from $(0,1)$ to $(k, \ell+1)$ and P_τ is from $(1,0)$ to $(k+1, \ell)$. This yields a cryptomorphic version of Theorem 3.1.

Theorem 3.2. *There is a bijection between full binary trees with $k+1$ left leaves and $\ell+1$ right leaves and pairs (P_β, P_α) of non-intersecting upright lattice paths, where P_β is from $(0,1)$ to $(\ell, k+1)$ and P_α is from $(1,0)$ to $(\ell+1, k)$.*

The advantage of working with non-intersecting lattice paths is that now we can apply the Lemma of Gessel-Viennot [27]; see also [2].

Theorem 3.3. *The number of full binary trees with $k+1$ left leaves and $\ell+1$ right leaves is*

$$\det \begin{pmatrix} \binom{k+\ell}{k} & \binom{k+\ell}{k-1} \\ \binom{k+\ell}{k+1} & \binom{k+\ell}{k} \end{pmatrix} = \frac{1}{k+\ell+1} \binom{k+\ell+1}{k} \binom{k+\ell+1}{k+1}$$

This is the *Narayana number* $N(k+\ell+1, k+1)$. From an elementary application of Vandermond's convolution, $\sum_{k=1}^{n-1} N(n,k) = \frac{1}{n}\binom{2n}{n-1} = C_n$. The following proposition summarizes our findings about Narayana families.

Narayana number

Proposition 3.2. The Narayana number $N(k+\ell+1, k+1)$ counts

- alternating trees with $k+1$ left vertices and $\ell+1$ right vertices,
- full binary trees with $k+1$ left leaves and $\ell+1$ right leaves,
- pairs (σ, τ) of $0,1$ strings in $\binom{k+\ell}{k}$ with $\tau \geq_{\mathsf{dom}} \sigma$,
- pairs (P_1, P_2) of non-intersecting upright lattice paths, where P_1 is from $(0,1)$ to $(k, \ell+1)$ and P_2 is from $(1,0)$ to $(k+1, \ell)$.

4 Twin Pairs of Trees and the Baxter Numbers

After the Catalan digression we come back to twin pairs of trees.

Definition 4.1. A pair (A, B) of full binary trees whose fingerprints satisfy $\hat{\alpha}(A) = \rho(\hat{\alpha}(B))$ is called a *twin-binary pair of trees.*

twin-binary pair of trees

Theorem 4.1. *There is a bijection between twin-alternating pairs of trees on n vertices and twin-binary pairs of trees with n leaves.*

Proof. Let (A, B) be twin-binary trees. Apply the correspondence from Proposition 3.1 to both. This yields trees S and T such that $\hat{\alpha}_\nearrow(S) = \hat{\alpha}(A)$ and $\hat{\alpha}_\nearrow(T) = \hat{\alpha}(B)$ and $S^\lambda = A$ and $T^\lambda = B$. From $\hat{\alpha}(A) = \rho(\hat{\alpha}(B))$ we conclude $\hat{\alpha}_\nearrow(S) = \rho(\hat{\alpha}_\nearrow(T))$ which is the defining property for twin-alternating trees. □

In the proof of Theorem 2.2 we have seen how a twin-alternating pair of trees can be extended and then glued together to yield a 2-book embedding of a quadrangulation; see also Figure 4. Doing a similar gluing for a twin-binary pair of trees, with both trees drawn as in the proof of Proposition 3.1, yields a particular rectangulation of the square. Figure 8 shows an example.

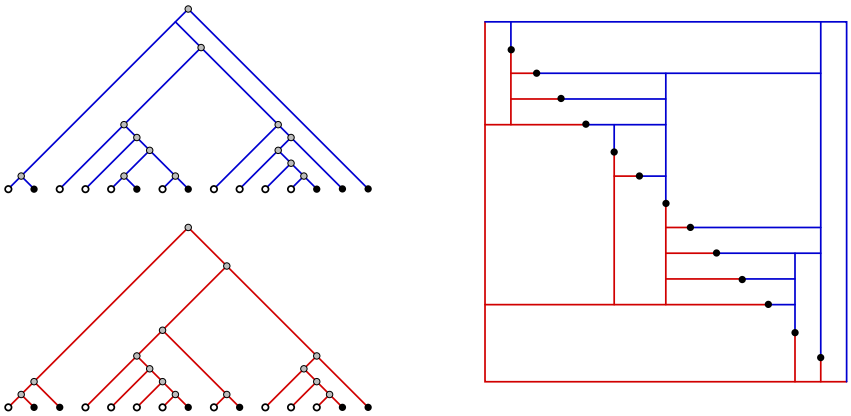

Figure 8: A twin-binary pair of trees and the associated rectangulation.

Definition 4.2. Let X be a set of points in the plane and let R be an axis-aligned rectangle which contains X in its open interior. A *rectangulation of* X is a subdivision of R into rectangles by non-crossing axis-parallel segments, such that every segment contains a point of X and every point lies on a segment.

rectangulation of X

We are mainly interested in rectangulations of diagonal sets, i.e., of the sets $X_{n-1} = \{(i, n-i) : 1 \leq i \leq n-2\}$. In this case the enclosing rectangle R can be chosen to be the square spanned by $(0,0)$ and (n,n). Figure 8 shows a rectangulation of X_{13}. The following theorem is immediate from the definitions.

Theorem 4.2. *There is a bijection between twin-binary pairs of trees with n leaves and rectangulations of X_{n-2}.*

Note.

Hartman et al. [29] and later independently de Fraysseix et al. [15] prove that it is possible to assign a set of internally disjoint vertical and horizontal segments to the vertices of any bipartite graph G such that two segments touch if, and only if, there is an edge between the corresponding vertices. A proof of this result can be given along the following line: Extend G by adding edges and vertices to a quadrangulation Q. Augment Q with a 2-orientation and trace the mappings from 2-orientations via twin-alternating pairs of trees to a rectangulation of a diagonal point set. The horizontal and vertical segments through the points are a touching segment representation for Q. Deleting some and retracting the ends of some other segments yields a representation for G. A similar observation was made by Ackerman, Barequet and Pinter [1].

Let (S,T) be a twin pair of binary trees with $k+1$ left and $\ell+1$ right leaves. The bijection from Theorem 3.2 maps $Y \in \{S,T\}$ to a pair $(P_\beta(Y), P_\alpha(Y))$ of non-intersecting upright lattice paths, where $P_\beta(Y)$ is from $(0,1)$ to $(\ell, k+1)$ and $P_\alpha(Y)$ is from $(1,0)$ to $(\ell+1, k)$. Since by definition $\hat{\alpha}(S) = \rho(\hat{\alpha}(T))$ a point reflection of $P_\alpha(T)$ at $(0,0)$ followed by a translation by $(\ell+2, k)$ maps $P_\alpha(T)$ to the path $P^*_\alpha(T)$ defined as $P^*_\alpha(T) = P_\alpha(S)$. The same geometric transformation maps $P_\beta(T)$ to $P^*_\beta(T)$ from $(2,-1)$ to $(\ell+2, k-1)$ and of course $(P^*_\beta(T), P^*_\alpha(T))$ is again a pair of non-intersecting upright lattice paths. Actually, $(P_\beta(S), P_\alpha(S), P^*_\beta(T)) = (P_\beta(S), P^*_\alpha(T), P^*_\beta(T))$ is a triple of non-intersecting upright lattice paths. Since the first two

of these paths uniquely determine S and the last two uniquely determine T we obtain, via a translation of the three paths one unit up, the following theorem.

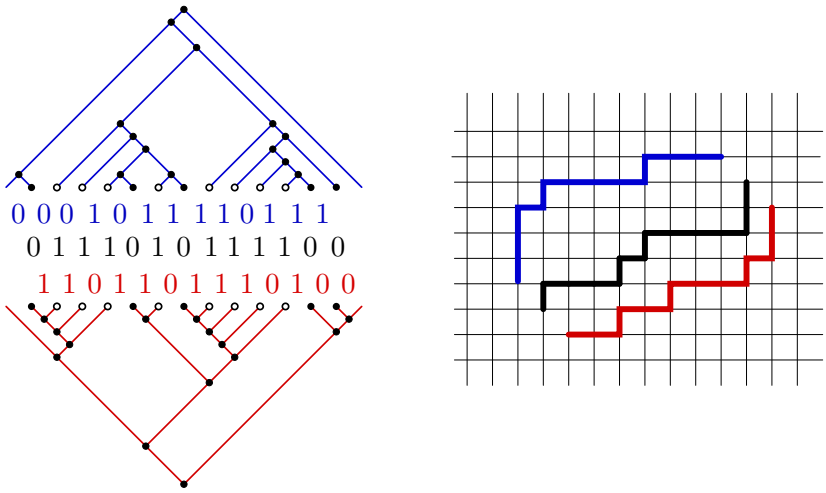

Figure 9: A twin-binary pair of trees and its triple of non-intersecting lattice paths.

Theorem 4.3. *There is a bijection between twin pairs of full binary trees with $k+1$ left leaves and $\ell+1$ right leaves and triples (P_1, P_2, P_3) of non-intersecting upright lattice paths, where P_1 is from $(0,2)$ to $(k, \ell+2)$, P_2 is from $(1,1)$ to $(k+1, \ell+1)$, and P_3 is from $(2,0)$ to $(k+2, \ell)$.*

Again we can apply the Lemma of Gessel-Viennot.

Theorem 4.4. *The number of twin pairs of full binary trees with $k+1$ left leaves and $\ell+1$ right leaves is*

$$\det\begin{pmatrix} \binom{k+\ell}{k} & \binom{k+\ell}{k-1} & \binom{k+\ell}{k-2} \\ \binom{k+\ell}{k+1} & \binom{k+\ell}{k} & \binom{k+\ell}{k-1} \\ \binom{k+\ell}{k+2} & \binom{k+\ell}{k+1} & \binom{k+\ell}{k} \end{pmatrix} = 2\,\frac{(k+\ell)!\,(k+\ell+1)!\,(k+\ell+2)!}{k!\,(k+1)!\,(k+2)!\,\ell!\,(\ell+1)!\,(\ell+2)!} = \Theta_{k,\ell}$$

The number $\Theta_{k,\ell}$ has some quite nice expressions in terms of binomial coefficients, e.g., $\Theta_{k,\ell} = \frac{2}{(k+1)^2\,(k+2)}\binom{k+\ell}{k}\binom{k+\ell+1}{k}\binom{k+\ell+2}{k}$ or $\Theta_{k,\ell} = \frac{2}{(n+1)\,(n+2)^2}\binom{k+\ell+2}{k}\binom{k+\ell+2}{k+1}\binom{k+\ell+2}{k+2}$. The total number of twin binary trees with $n+2$ leaves is given by the *Baxter number*

Baxter number

$$B_{n+1} = \sum_{k=0}^{n} \Theta_{k,n-k},$$

whose initial values are $1, 2, 6, 22, 92, 422, 2074, 10754$. The next proposition collects families that are, due to our bijections, enumerated by Θ-numbers.

Proposition 4.1. The number $\Theta_{k,\ell}$ counts

- triples (P_1, P_2, P_3) of non-intersecting upright lattice paths, where P_1 is from $(0,2)$ to $(\ell, k+2)$ and P_2 is from $(1,1)$ to $(\ell+1, k+1)$ and P_3 is from $(2,0)$ to $(\ell+2, k)$.
- twin pairs of binary trees with $k+1$ left leaves and $\ell+1$ right leaves,

- rectangulations of $X_{k+\ell}$ with k horizontal and ℓ vertical segments,
- twin pairs of alternating trees with $k+1$ left vertices and $\ell+1$ right vertices,
- separating decompositions of quadrangulations with $k+2$ white and $\ell+2$ black vertices,
- 2-orientations of quadrangulations with $k+2$ white and $\ell+2$ black vertices.

Note.

The concept of twin-binary pairs of trees is due to Dulucq and Guibert [18]. They also give a bijection between twin-binary pairs of trees and triples of non-intersecting lattice paths. The bijection also uses the fingerprint as the middle path, the other two are defined differently. In [19] they extend their work to include some more refined counts. A very good entrance point for more information about Baxter numbers is The On-Line Encyclopedia of Integer Sequences [39, A001181].

Fusy, Schaeffer and Poulalhon [25] gave a direct bijection from separating decompositions to triples of non-intersecting paths in a grid. Their main application is the counting of bipolar orientations of rooted 2-connected maps. These results are included in Section 5.2.

Ackerman, Barequet and Pinter [1] also have the result that the number of rectangulations of X_n is the Baxter number B_{n+1}. Their proof is via a recurrence formula obtained by Chung et al. [12]. They also show that for a point set $X_\pi = \{(i, \pi(i)) : 1 \leq i \leq n\}$ to have exactly B_{n+1} rectangulations it is sufficient that π is a Schröder permutation, i.e., a permutation avoiding the patterns $3-1-4-2$ and $2-4-1-3$. They conjecture that whenever π is a permutation that is not Schröder, the number of rectangulations of X_π is strictly larger than the Baxter number.

In contrast to the nice formulas for the number of 2-orientations of quadrangulations on n vertices, very little is known about the number of 2-orientations of a fixed quadrangulation Q. In [22] it is shown that the maximal number of 2-orientations a quadrangulation on n vertices can have is asymptotically between $1,47^n$ and $1,91^n$. To our knowledge, the computational complexity of the counting problem is open.

5 More Baxter Families

In this section we deal with Baxter permutations and bipolar orientations. In both families we identify objects counted by Θ-numbers and less refined families counted by Baxter numbers.

5.1 Baxter Permutations

Definition 5.1. The *max-tree* $\mathsf{Max}(\pi)$ of a permutation π is recursively defined as the binary tree with root labeled z, left subtree $\mathsf{Max}(\pi_{\text{left}})$ and right subtree $\mathsf{Max}(\pi_{\text{right}})$ where z is the maximum entry of π and in one-line notation $\pi = \pi_{\text{left}}, z, \pi_{\text{right}}$. The recursion ends with unlabeled leaf-nodes corresponding to $\mathsf{Max}(\emptyset)$. *max-tree*

The max-tree of a permutation is a full binary tree. The ith leaf v_i of $\mathsf{Max}(\pi)$ from the left corresponds to the adjacent pair (π_{i-1}, π_i) in the permutation π. Leaf v_i is a left leaf if, and only if, (π_{i-1}, π_i) is a descent, i.e., if $\pi_{i-1} > \pi_i$.

The *min-tree* $\mathsf{Min}(\pi)$ of a permutation π is defined dually, i.e., as the binary tree with root labeled a, left subtree $\mathsf{Min}(\pi_{\text{left}})$ and right subtree $\mathsf{Min}(\pi_{\text{right}})$ where a is the minimum entry *min-tree*

of $\pi = \pi_{\text{left}}, a, \pi_{\text{right}}$. Also let $\mathsf{Min}(\emptyset)$ be a leaf-node. The ith leaf y_i of $\mathsf{Min}(\pi)$ from the left is a left leaf if, and only if, (π_{i-1}, π_i) is a rise, i.e., if $\pi_{i-1} < \pi_i$.

With these definitions and observations, see also Figure 10, we obtain:

Proposition 5.1. For a permutation π of $[n-1]$ the pair $(\mathsf{Max}(\pi), \mathsf{Min}(\rho(\pi)))$ is a twin binary pair of trees.

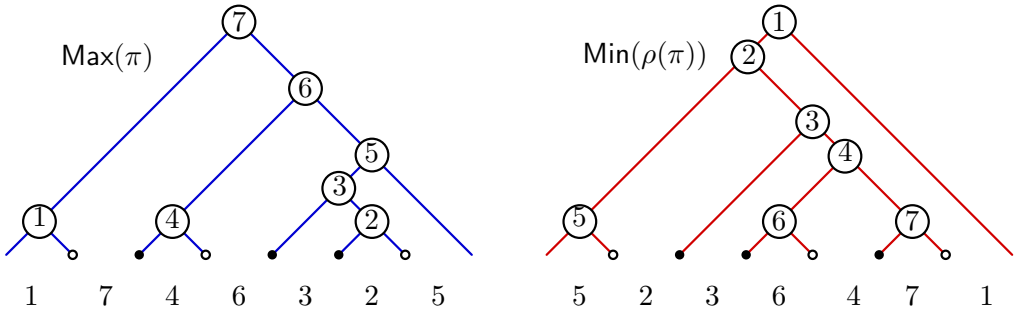

Figure 10: The trees $\mathsf{Max}(\pi)$ and $\mathsf{Min}(\rho(\pi))$ associated with $\pi = 1, 7, 4, 6, 3, 2, 5$.

This mapping from permutations to twin binary pairs of trees is not a bijection. Indeed, the permutation $\pi' = 1, 7, 5, 6, 3, 2, 4$ also maps to the pair of trees shown in Figure 10.

Definition 5.2. A *Baxter permutation* is a permutation which avoids the pattern 2–41–3 and 3–14–2. That is, π is Baxter if there are no indices $i < j, j+1 < k$ with $\pi_{j+1} < \pi_i < \pi_k < \pi_j$ nor with $\pi_{j+1} > \pi_i > \pi_k > \pi_j$. *Baxter permutation*

Theorem 5.1. *There is a bijection between twin binary trees with n leaves and Baxter permutations of $[n-1]$.*

Proof. From Proposition 5.1 we know that $(\mathsf{Max}(\pi), \mathsf{Min}(\rho(\pi)))$ is a twin binary pair of trees; this remains true if we restrict π to be Baxter.

For the converse let (S, T) be twin binary trees with n leaves. With this pair associate a rectangulation of X_{n-2}. Tilt the rectangulation to get the diagonal points onto the x-axis. Each rectangle of the rectangulation contains a highest corner which corresponds to an inner vertex of S and a lowest corner corresponding to an inner vertex of T. We will refer to these corners as the *north-corner* and the *south-corner* respectively. *north-corner* *south-corner*

The idea is to associate a number with every rectangle; the permutation π corresponding to (S, T) is then read of from the order of intersection of the rectangles with the x-axis. Writing the numbers of rectangles to their north- and south-corners makes $(S, T) = (\mathsf{Max}(\pi), \mathsf{Min}(\rho(\pi)))$.

The algorithm associates the numbers with rectangles in decreasing order. Number $n-1$ is associated with the rectangle with highest north-corner. After having associated k with some rectangle R_k, the union of unlabeled rectangles can be seen as a series of pyramids over the x-axis; see Figure 11.

The label $k-1$ has to correspond to one of the rectangles which have their north-corner on the tip of one of the pyramids (this is because S will be the max-tree of π). The algorithm will choose the next pyramid to the left or the next pyramid to the right of the interval on the x-axis which belongs to R_k. The decision which of the two is taken depends on the south-corner of R_k. If the south-corner is a ⟍, i.e., a left child in tree T, then the pyramid to the left is chosen; otherwise, if the south-corner is a ⟋, then the pyramid to the right is chosen.

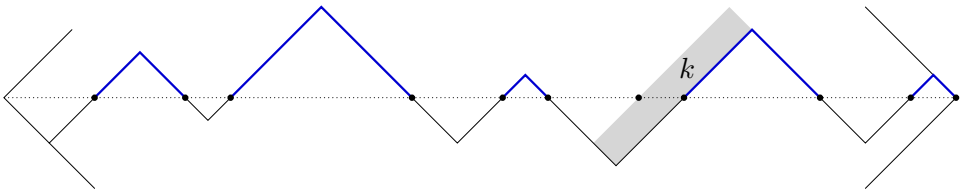

Figure 11: A series of pyramids after labeling rectangle k.

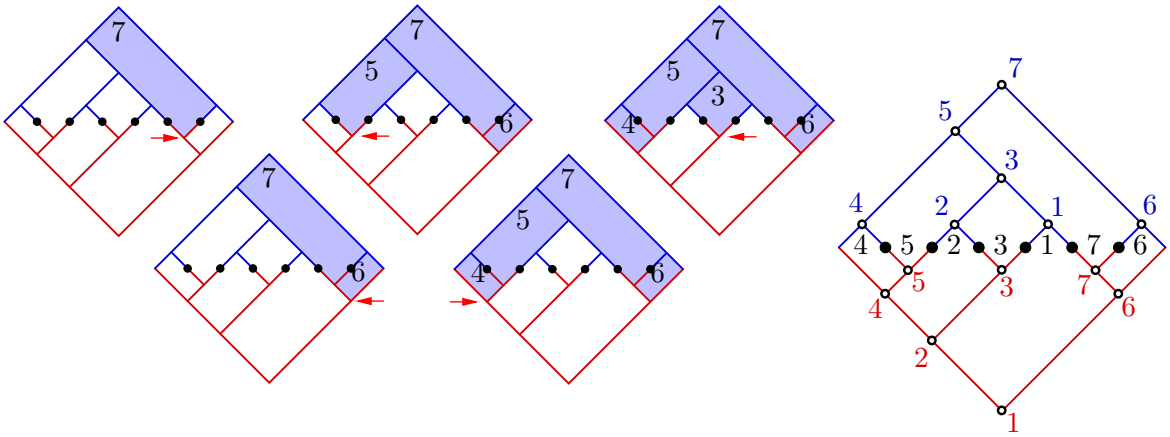

Figure 12: Generating a Baxter permutation from a rectangulation. The final state shows the permutation with its max- and min-trees.

An example for the execution of this algorithm is given in Figure 12. The proof that this is a bijection is done with three claims.

Claim A. The permutation constructed by the algorithm is Baxter.

Proof of the claim. Let $a < b < c < d$, we want to show that the algorithm will not produce the pattern b–da–c. Think of the status after labeling rectangle $R(c)$. To have a chance of producing the pattern d is left of c and the slot immediately to the right of d is not yet used, i.e., it belongs to a pyramid P. From the labeling rule of the algorithm it follows that the rectangle covering the leftmost slot of P has to be labeled before any rectangle left of P can be labeled. This shows that the pattern is impossible. The case of the other pattern is symmetric. △

Claim B. The border between labeled and unlabeled rectangles at any stage of the algorithm is a zig-zag (the definition of zig-zag should be evident from Figure 11).

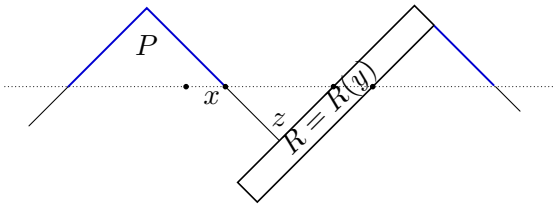

Figure 13: A violation of the zig-zag property.

Proof of the claim. Suppose not. Then there is a first rectangle R whose labeling violates the property, Figure 13 shows the situation up to a reflection interchanging left and right. Let y be the label of R and let z be the label of the rectangle whose south-corner is the deepest point of the valley whose shape was destroyed by $R(y)$. The rule of the algorithm implies that the rectangle labeled after z was left of $R(z)$. This rectangle $R(z-1)$ has to intersect the x-axis somewhere left of pyramid P. From the labeling rule of the algorithm it follows that the rectangle covering the rightmost slot of P has to be labeled before any rectangle right of P can be labeled. Rectangle R however is right of P, a contradiction. △

Claim B implies that in the lower tree the labels of south-corners of rectangles are decreasing along every path from a leaf to the root. This is a property characterizing Min-trees, hence, the labels of the rectangles yield the $\mathsf{Min}(\rho(\pi))$. The fact that the labeling of the north-corners of rectangles yields the $\mathsf{Max}(\pi)$ is more immediate from the algorithm.

Claim C. If σ is a permutation with $(\mathsf{Max}(\sigma), \mathsf{Min}(\rho(\sigma))) = (S, T)$ and σ is not the result of applying the algorithm to the rectangulation corresponding to (S, T), then σ is not Baxter.

Proof of the claim. Compare the one-line notation of σ and π, where π is the result of applying the algorithm to the rectangulation corresponding to (S, T). Consider the largest value k which is not at the same position in σ and π. Clearly $k \neq n-1$, because σ and π have the same max-tree. Hence, if we think of the algorithm producing π in the state when $k+1$ is placed, then the placement of k in σ fails to obey the rules of the algorithm. Either k is placed as to have its north-corner in a pyramid on the wrong side, or the side is respected but the pyramid containing the north-corner of k is not next to $R(k+1)$ on this side. We indicate how to find a forbidden pattern in each of the two cases.

Wrong side. Suppose the south-corner p of $R(k+1)$ is a ↘ and k is placed to the right of $k+1$. Let a be the element in σ whose rectangle has its east-corner at p and let q be the first node of type ↙ on the path from p to the root of the min-tree, i.e, of T. Let b be the element in σ whose rectangle has its west-corner at q. From the min-tree property we infer that $b < a < k$. Since $k+1$ and b are neighbors in σ, the elements $a, k+1, b, k$ form a forbidden 3–14–2 pattern.

The other case where the south-corner p of $R(k+1)$ is a ↙ is symmetric. In this case there is a forbidden pattern 2–41–3.

Wrong pyramid. Suppose the south-corner p of $R(k+1)$ is a ↘ and k is placed to a pyramid left of $k+1$ but not to the first one. Let $r > k+1$ be some element separating the first from the second pyramid. Let a be the element in σ whose rectangle has its east-corner at p and note that $a < k$. Between r and a there is an adjacent pair r', a' with $a' < k$ and $k+1 < r'$. Hence, $k, r', a', k+1$ is a forbidden 2–41–3. Again, the second case is symmetric. This completes the proof of the claim △

Claim A says that every twin binary pair (S, T) of trees is mapped by the algorithm to a Baxter permutation π. As a consequence of Claim B we noted that $(S, T) = (\mathsf{Max}(\pi), \mathsf{Min}(\rho(\pi))$. Claim C is the injectivity, hence, the mapping is a bijection. □

From Proposition 4.1 and the observation about the correspondence of left and right leaves in the max-tree of a permutation with descents and rises we obtain:

Proposition 5.2. The number $\Theta_{k,\ell}$ counts

- twin pairs of binary trees with $k+1$ left leaves and $\ell+1$ right leaves,
- Baxter permutations of $k+\ell+1$ with k descents and ℓ rises.

Note.

Baxter numbers first appeared in the context of counting Baxter permutations. Chung, Graham, Hoggatt and Kleiman [12] found some interesting recurrences and gave a proof based on generating functions. Mallows [33] found the refined count of Baxter permutations by rises (Proposition 5.2). The bijection of Theorem 5.1 is essentially due to Dulucq and Guibert [18, 19]. Their description and proof, however, does not use geometry. They also prove Proposition 5.2 and some even more refined counts, e.g., the number of Baxter permutations of $[n]$ with ℓ rises and s left-to-right maxima and t right-to-left maxima.

alternating

A permutation $(a_1, a_2, \ldots, a_n)$ is *alternating* if $a_1 < a_2 > a_3 < a_4 > \ldots$, i.e., each consecutive pair a_{2i-1}, a_{2i} is a rise and each pair a_{2i}, a_{2i+1} a descent. Alternating permutations are characterized by the property that the reduced fingerprints of their Min- and Max-trees are alternating, i.e., of the form $\ldots 0, 1, 0, 1, 0, 1, \ldots$ and in addition, to ensure that the first pair is a rise, the first entry of the reduced fingerprints of the Max-tree is a 0. Due to this characterization we obtain the following specialization of Theorem 5.1:

Lemma 5.1. *Twin pairs of binary trees with an alternating reduced fingerprint starting in 0 and alternating Baxter permutations are in bijection.*

Let T be a binary tree with n leaves and with an alternating reduced fingerprint starting with a 0. The leaves of T come in pairs from left to right so that the leaves from each pair are attached to the same interior node. Pruning the leaves we obtain a tree T' with $n - \lfloor \frac{n}{2} \rfloor$ leaves. From T' we come back to T by attaching a new pair of leaves to each of the first $\lfloor \frac{n}{2} \rfloor$ leaves of T'. Using this kind of bijection we obtain two bijections (see Figure 14):

- a bijection between alternating Baxter permutations of $[2k-1]$ and pairs of binary trees with k leaves, and
- a bijection between alternating Baxter permutations of $[2k]$ and pairs of binary trees with k and $k+1$ leaves.

Theorem 5.2. *The number of alternating Baxter permutations on $[n-1]$ is $C_{k-1}C_k$ if $n = 2k$ and $C_{k-1}C_{k-1}$ if $n = 2k-1$.*

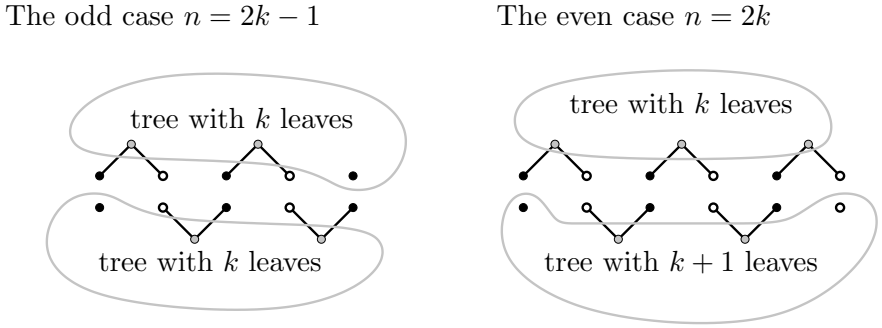

Figure 14: Alternating Baxter permutations and pairs of trees.

Note.

Theorem 5.2 was obtained by Cori et al. [13]. It was reproved by Dulucq and Guibert [18] as a specialization of their bijection between Baxter permutations and twin pairs of binary trees. In [28] it is shown that alternating Baxter permutations with the property that their inverse is again alternating Baxter are counted by the Catalan numbers.

5.2 Plane Bipolar Orientations

A graph G is said to be *rooted* if one of its edges is distinguished and oriented. The origin and the end of the root-edge are denoted s and t. If G is a *plane graph*, the root-edge is always assumed to be incident to the outer face, with the outer face on its left.

Definition 5.3. A *bipolar orientation* of a rooted graph G is an acyclic orientation of G such that the unique source (i.e., vertex with only outgoing edges) is s and the unique sink (i.e., vertex with only ingoing edges) is t. A *plane bipolar orientation* is a bipolar orientation on a rooted plane graph (multiple edges are allowed). *bipolar orientation*

It is well-known that the rooted graphs admitting a bipolar orientation are exactly 2-connected graphs, i.e., graphs with no separating vertex.

Note.

Bipolar orientations have proved to be insightful in solving many algorithmic problems such as planar graph embedding [31, 11] and geometric representations of graphs in various flavors (visibility [41], floor planning [35, 30], straight-line drawing [42, 23]). They also constitute a beautiful combinatorial structure; the thesis of Ossona de Mendez is devoted to studying their numerous properties and applications [17]; see also [16] for a detailed survey.

Let G be a rooted plane graph; the *angular map* of G is the graph Q with vertex set consisting of vertices and faces of G, and edges corresponding to incidences between a vertex and a face. The special vertices s, t of Q are the extremities (origin s and end t) of the root-edge of G. *angular map*

The angular map Q of G inherits a plane embedding from G. The unique bipartition of Q has the vertices of G in one color class and the faces of G in the other. We assume that vertices of G are black and faces of G are white. All the faces of Q are quadrangles, which correspond to the edges of G. Moreover, since G is 2-connected, Q has no double edges, so Q is a quadrangulation.

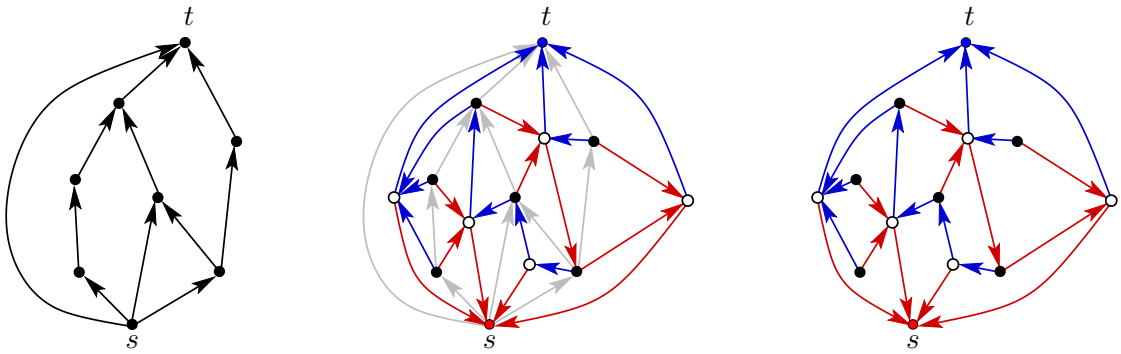

Figure 15: From a rooted map endowed with a bipolar orientation to a separating decomposition on the angular map.

If G is endowed with a bipolar orientation B, the angular map can be enriched in order to transfer the orientation onto Q. Actually, we will define a bijection between bipolar orientations of G and separating decompositions of Q. The construction, based on two facts about bipolar orientations of rooted plane graphs, is illustrated in Figure 15.

Fact V. Every vertex $v \neq s, t$ has exactly two adjacent faces (angles) where the orientation of the edges differ.

Fact F. Every face f has exactly two vertices (angles) where the orientation of the edges coincide.

Facts V and F specify two distinguished edges in the angular map for every non-special vertex and every face. Since every edge of Q is distinguished either for a vertex or for a face this yields a 2-orientation. Figure 16 indicates how to color this 2-orientation to get a separating decomposition on Q. From a separating decomposition on Q, the unique bipolar orientation on G inducing Q is easily recovered. (If Q has white vertices of degree 2, then there are multi-edges on G). To summarize:

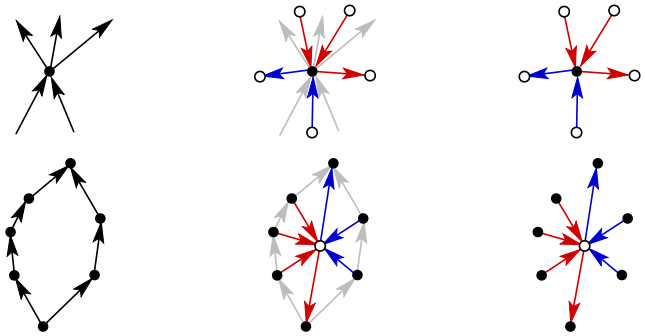

Figure 16: The transformation for a vertex and a face of a rooted map.

Proposition 5.3. Plane bipolar orientations with $\ell+2$ vertices and $k+2$ faces are in bijection with separating decompositions of quadrangulations with $\ell+2$ black vertices and $k+2$ white vertices. Consequently, the number $\Theta_{k,\ell}$ counts:

- separating decompositions of quadrangulations with $k+2$ white and $\ell+2$ black vertices,
- Bipolar orientations of rooted plane graphs with $k+2$ faces and $\ell+2$ vertices.

In Section 7 we will use this and some previous bijections to give an independent proof for a beautiful formula of Bonichon [7] for the number of Schnyder woods on triangulations with n vertices.

Note.

The two facts **V** and **F** have been rediscovered frequently, they can be found, e.g., in [16, 35, 41]. Actually, plane bipolar orientations can be defined via properties **V** and **F**. The bijection of Proposition 5.3 is a direct extension of [16, Theo 5.3]. In 2001, R. Baxter [5, Eq 5.3] guessed that plane bipolar orientations are counted by the Θ-numbers. His verification is based on algebraic manipulations on generating functions of plane graphs weighted by their Tutte polynomials. A simpler proof for this fact was obtained by Fusy et al. [25] via a direct bijection from separating decompositions to triples of non-intersecting lattice paths. Their bijection presents significant differences from the one presented in this article, even if the classes in correspondence are the same. The main difference is that they do not treat the blue tree and the red tree of a separating decomposition in a symmetric way, as we do here, and their correspondence is less geometric. (In their bijection, the blue tree is encoded as a refined Dyck word, while the red edges are encoded as the sequence of degrees in red of the white vertices.)

As shown in [16], the number of bipolar orientations of a fixed rooted graph G is equal to twice the coefficient $[x]T_G(x,y)$ in the Tutte polynomial of G. This coefficient is called

Crapo's β invariant and it is #P-hard to compute [3]. To our knowledge, the computational complexity of the counting problem restricted to rooted *plane* graphs is open. (By the angular map bijection, it is clearly equivalent to computing the number of 2-orientations of a fixed quadrangulation.)

5.3 Digression: Duality, Completion Graph, and Hamiltonicity

duality mapping

There exists a well-known *duality mapping* for plane graphs. The dual G^* of a plane graph G has its vertices corresponding to the faces of G, and has its edges corresponding to the adjacencies of the faces of G (two faces are adjacent if they share an edge). Precisely, each edge e of G gives rise to an edge e^* of G^* that connects the vertices of G^* corresponding to the faces of G on each side of e. Let us mention here, even if we do not make use of this fact, that duality can be enriched to take account of bipolar orientations [16]; if G is endowed with a bipolar orientation, each (oriented) non-root edge e of G gives rise to an oriented edge e^* of G^* that goes from the face on the left to the face on the right of e (for the root edge the opposite rule has to be applied).

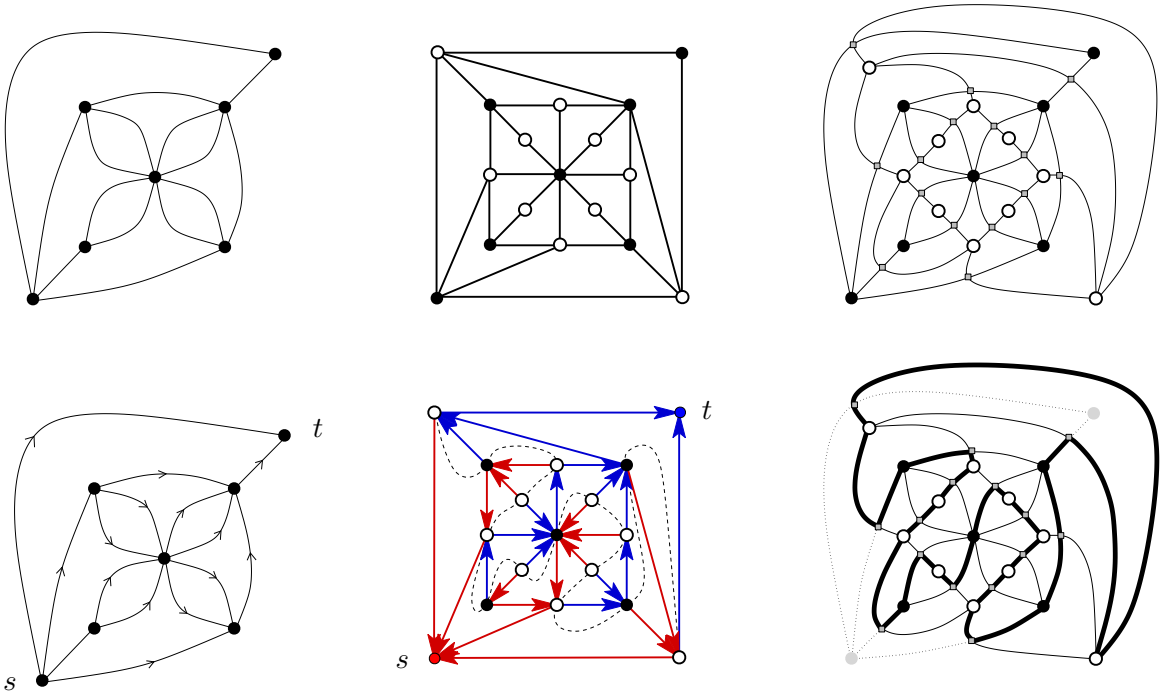

Figure 17: Top, from left to right: A 2-connected plane graph, its quadrangulation, and its completion graph. Bottom, from left to right: the same 2-connected plane graph rooted at an edge and endowed with a bipolar orientation, the quadrangulation endowed with the corresponding separating decomposition (the equatorial line of the 2-book embedding is drawn —in dashed line— by bisecting all bicolored angles), and the special completion graph endowed with the corresponding Hamiltonian cycle.

completion graph
primal vertices
dual vertices
edge-vertices

The *completion graph* $\widetilde{G}$ of G is the plane graph obtained by superimposing G and its dual G^*, see Figure 17. Vertices of $\widetilde{G}$ are of 3 types: *primal vertices* are the vertices of G, *dual vertices* are the vertices of G^*, and *edge-vertices* are the vertices at the intersection of

an edge $e \in G$ with its dual edge e^* (hence edge-vertices have degree 4 in $\widetilde{G}$). Observe in Figure 17 that the completion graph of G and the quadrangulation Q of G differ only upon replacing the contour of each face f of Q by a 4-star, the extremities of the 4-star being the 4 vertices incident to f and the center of the 4-star being the edge-vertex of $\widetilde{G}$ associated with f (each edge of G corresponds both to a face of Q and to an edge-vertex of $\widetilde{G}$, which yields a correspondence between faces of Q and edge-vertices of $\widetilde{G}$).

If G is rooted, the origin s and end t of the root-edge are the *special vertices* of G; the *special completion graph* of G is the plane graph obtained from $\widetilde{G}$ by removing s and t as well as their incident edges.

special vertices

special completion graph

Proposition 5.4. The special completion graph of a rooted 2-connected plane graph is Hamiltonian.

Proof. Given G a rooted 2-connected plane graph, we first endow G with a bipolar orientation, and consider the quadrangulation Q of G endowed with the corresponding separating decomposition S. As proved in Lemma 2.1), the equatorial line of S is a simple path that has the two outer nonspecial vertices as extremities and passes once by each inner vertex and once by the interior of each inner face of Q. By the above discussion on the correspondence between Q and $\widetilde{G}$, the path is easily deformed to a simple path on the graph $\widetilde{G}$ visiting once all the vertices of $\widetilde{G}$ except the two special ones, see Figure 17. In addition, the path does not use the 4-star of $\widetilde{G}$ corresponding to the outer face of f. Completing the path with the two edges of the outer 4-star incident to white vertices, we obtain a Hamiltonian cycle of the special completion graph. □

6 Symmetries

As we explain in this section, the bijections we have presented have the nice property that they commute with the half-turn rotation, which makes it possible to count *symmetric* combinatorial structures. The first structures we have encountered are 2-orientations. Given a 2-orientation O, exchanging the two special vertices $\{s, t\}$ of O clearly yields another 2-orientation, which we call the *pole-inverted* 2-orientation of O and denote by $\iota(O)$. A 2-orientation is called *pole-symmetric* if O and $\iota(O)$ are isomorphic.

pole-inverted

pole-symmetric

Considering the associated separating decomposition, the blue tree of O is the red tree of $\iota(O)$ and vice versa. Accordingly, a 2-orientation is pole-symmetric if, and only if, the blue tree and the red tree are isomorphic as rooted trees, in which case the separating decomposition is called pole-symmetric as well. Such a symmetry translates to half-turn rotation symmetries on the associated embeddings. Indeed, as the two trees composing the separating decomposition are isomorphic, so are their alternating embeddings and so are the two binary trees that compose the associated twin pair of full binary trees, in which case the twin pair is called *symmetric*. Hence, the 2-book embedding and rectangulation associated with the separating decomposition are stable under the half-turn rotation that exchanges the two special vertices. Such 2-book embeddings and rectangulations are called *pole-symmetric* as well.

Considering Baxter permutations, the min-tree (resp., max-tree) of a Baxter permutation π is the max-tree (resp., min-tree) of the associated Baxter permutation $\overline{\rho(\pi)}$, i.e., the permutation whose 0-1 matrix is the 0-1 matrix of π after half-turn rotation. Baxter permutations for which $\pi = \overline{\rho(\pi)}$ are said to be *symmetric*. By definition of the bijective correspondence of

Theorem 5.1, a Baxter permutation is symmetric if, and only if, the associated twin pair of full binary trees is symmetric.

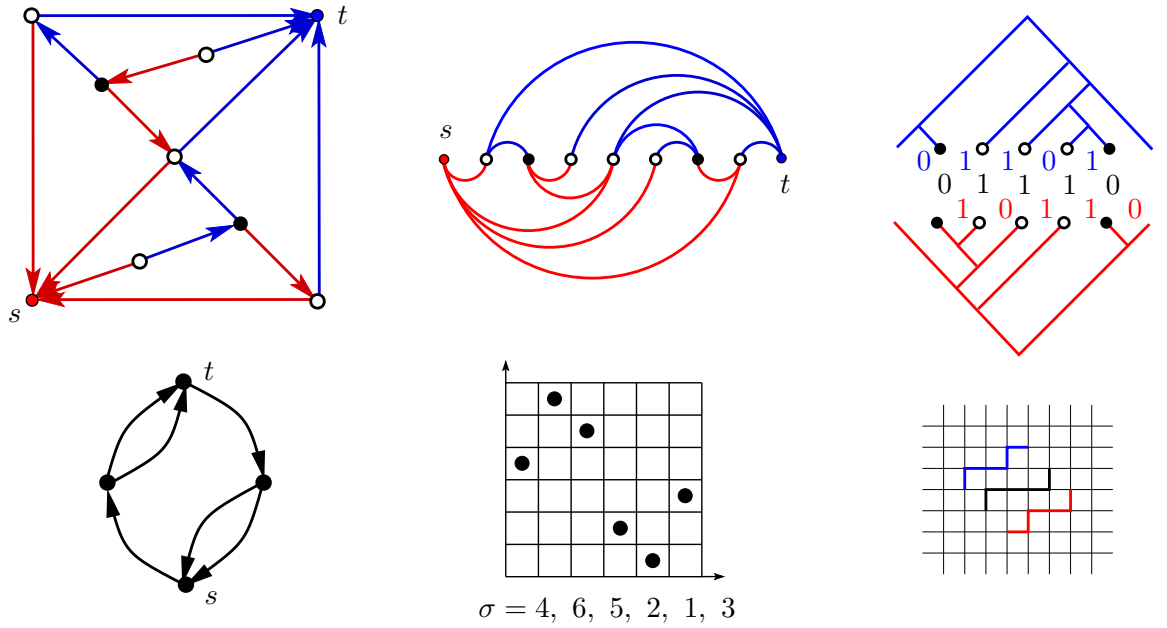

Figure 18: A pole-symmetric separating decomposition and the corresponding symmetric combinatorial structures: 2-book embedding, twin pair of full binary trees, plane bipolar orientation, Baxter permutation, triple of paths.

Next we turn to the encoding by a triple of paths. Recall that, in a twin pair (T, T') of full binary trees, the reduced fingerprints satisfy the relation $\hat{\alpha}(T) = \rho(\hat{\alpha}(T'))$. Hence, a symmetric twin pair (T, T) is characterized by the property that the reduced fingerprint of T satisfies $\hat{\alpha}(T) = \rho(\hat{\alpha}(T))$, i.e., $\hat{\alpha}$ is a palindrome. Equivalently, if T has $k+1$ left leaves and $\ell+1$ right leaves, the upright lattice path $P_2 := P_\alpha(T)$, as defined in Section 4, is stable under the point-reflection π_S at $S := (k/2+1, \ell/2+1)$. The other two paths in the triple (P_1, P_2, P_3) of non-intersecting lattice paths correspond to two copies of the bodyprint of T read respectively from $(0,2)$ to $(k, \ell+2)$ for P_1 and from $(\ell+2, k)$ to $(2,0)$ for P_3. Therefore the whole triple (P_1, P_2, P_3) is stable under the point reflection π_S. Such a triple of paths is called *symmetric*.

Lemma 6.1. *Let $\Theta^{\circlearrowleft}_{k,\ell}$ be the number of symmetric non-intersecting triples of upright lattice paths (P_1, P_2, P_3) going respectively from $(0,2)$, $(1,1)$, $(2,0)$ to $(k, \ell+2)$, $(k+1, \ell+1)$, $(k+2, \ell)$.*

(i) If k and ℓ are odd, then $\Theta^{\circlearrowleft}_{k,\ell} = 0$.

(ii) If k and ℓ are even, $k = 2\kappa$, $\ell = 2\lambda$, then

$$\Theta^{\circlearrowleft}_{k,\ell} = \sum_{r \geq 1} \frac{2r^3}{(\kappa+\lambda+1)(\kappa+\lambda+2)^2} \binom{\kappa+\lambda+2}{\kappa+1} \binom{\kappa+\lambda+2}{\kappa-r+1} \binom{\kappa+\lambda+2}{\kappa+r+1}.$$

(iii) If k is odd and ℓ is even, $k = 2\kappa+1$, $\ell = 2\lambda$, then

$$\Theta^{\circlearrowleft}_{k,\ell} = \sum_{r \geq 1} \frac{2r^3+(\lambda-r+1)r(r+1)(2r+1)}{(\kappa+\lambda+1)(\kappa+\lambda+2)^2} \binom{\kappa+\lambda+2}{\kappa+1} \binom{\kappa+\lambda+2}{\kappa-r+1} \binom{\kappa+\lambda+2}{\kappa+r+1}.$$

(iv) If k is even and ℓ is odd, $k = 2\kappa$, $\ell = 2\lambda + 1$, then

$$\Theta^{\circlearrowleft}_{k,\ell} = \sum_{r\geq 1} \frac{2r^3+(\kappa-r+1)r(r+1)(2r+1)}{(\kappa+\lambda+1)(\kappa+\lambda+2)^2} \binom{\kappa+\lambda+2}{\kappa+1}\binom{\kappa+\lambda+2}{\kappa-r+1}\binom{\kappa+\lambda+2}{\kappa+r+1}.$$

Proof. By definition, (P_1, P_2, P_3) is stable under the point-reflection π_S at $S := (\ell/2+1, k/2+1)$. In particular, P_2 is stable under π_S, so that P_2 has to pass by S. This can only occur if S is on an axis-coordinate, i.e., $k/2$ or $\ell/2$ are integers. Therefore $\Theta^{\circlearrowleft}_{k,\ell} = 0$ if both k and ℓ are odd.

If k and ℓ are even, $k = 2\kappa$ and $\ell = 2\lambda$, the half-turn symmetry ensures that P_1, P_2, P_3 is completely encoded upon keeping the part P'_1, P'_2, P'_3 of the paths that lie in the half-plane $\{x + y \leq x_S + y_S\}$, i.e., the half-plane $\{x + y \leq \kappa + \lambda + 2\}$. The conditions on (P_1, P_2, P_3) translate to the following conditions on the reduced triple: (P'_1, P'_2, P'_3) is non-intersecting, has same starting points as (P_1, P_2, P_3), the endpoint of P'_2 is S, and the endpoints of P'_1 and P'_3 are equidistant from S, i.e., there exists an integer $r \geq 1$ such that P'_1 ends at $(\kappa+1-r, \lambda+1+r)$ and P'_3 ends at $(\kappa+1+r, \lambda+1-r)$. Hence, up to fixing $r \geq 1$, (P'_1, P'_2, P'_3) form a non-intersecting triple with explicit fixed endpoints, so that the number of such triples can be expressed using Gessel-Viennot determinant formula. The expression for $\Theta^{\circlearrowleft}_{k,\ell}$ follows.

If k is odd and ℓ is even, $k = 2\kappa+1$ and $\ell = 2\lambda$, the triple (P_1, P_2, P_3) is again completely encoded by keeping the part (P'_1, P'_2, P'_3) of the paths that lie in $\{x + y \leq x_S + y_S\}$, i.e., the half-plane $\{x + y \leq \kappa + \lambda + 5/2\}$. The difference with the case where k and ℓ are even is that P'_1, P'_2, P'_3 are not standard lattice paths, as they end with a step of length $1/2$. Similarly as before, the conditions on (P_1, P_2, P_3) are equivalent to the properties that (P'_1, P'_2, P'_3) are non-intersecting, have the same starting points as (P_1, P_2, P_3), P'_2 ends at S, and P'_1, P'_3 end at points that are equidistant from S on the line $\{x + y = x_S + y_S\}$ and have one integer coordinate, i.e., there exists an integer $m \geq 2$ such that P'_1 ends at $(x_S - m/2, y_S + m/2)$ and P'_3 ends at $(x_S + m/2, y_S - m/2)$. Notice that, upon discarding the last step, the system (P'_1, P'_2, P'_3) is equivalent to a triple of non-intersecting upright lattice paths $(\overline{P'_1}, \overline{P'_2}, \overline{P'_3})$ with starting points $(0, 2)$, $(1, 1)$, $(2, 0)$, and endpoints that are either of the form $(\kappa+1-r, \lambda+1+r)$, $(\kappa+1, \lambda+1)$, $(\kappa+1+r, \lambda+1-r)$ if m is even, $m = 2r$, or are of the form $(\kappa+1-r, \lambda+1+r)$, $(\kappa + 1, \lambda + 1)$, $(\kappa + 2 + r, \lambda - r)$ if m is odd, $m = 2r + 1$. In each case, the number of triples has an explicit form from the formula of Gessel-Viennot. The expression of $\Theta^{\circlearrowleft}_{k,\ell}$ follows. Finally, notice that the set of symmetric non-intersecting triples is stable under swapping x-coordinates and y-coordinates, yielding the relation $\Theta^{\circlearrowleft}_{k,\ell} = \Theta^{\circlearrowleft}_{\ell,k}$. Thus the formula for $\Theta^{\circlearrowleft}_{k,\ell}$ when k is even and ℓ is odd simply follows from the formula obtained when k is odd and ℓ is even. □

Considering bipolar orientations, the effect of the half-turn symmetry of a separating decomposition on the associated plane bipolar orientation is clearly that the orientation is unchanged when the poles are exchanged, the directions of all edges are reversed, and the root-edge is flipped to the other side of the outer face (in fact it is more convenient to forget about the root-edge here). Such bipolar orientations are called *pole-symmetric*. The whole discussion on symmetric structures is summarized in the following proposition and illustrated in Figure 18.

Proposition 6.1. The number $\Theta^{\circlearrowleft}_{k,\ell}$ counts

- pole-symmetric 2-orientations with $k + 1$ white vertices and $\ell + 1$ black vertices,

- pole-symmetric separating decompositions and 2-book embeddings with $k+1$ white vertices and $\ell+1$ black vertices,
- symmetric twin pairs of full binary trees with $k+1$ left leaves and $\ell+1$ right leaves,
- pole-symmetric rectangulations of X_n with k horizontal and ℓ vertical segments
- symmetric Baxter permutations of $k+\ell+1$ with k descents and ℓ rises,
- pole-symmetric plane bipolar orientations with k inner faces and ℓ non-pole vertices.

7 Schnyder Families

Baxter numbers count 2-orientations on quadrangulations and several other structures. We now turn to a family of structures which are equinumerous with 3-orientations of plane triangulations.

Consider a plane triangulation T, i.e., a maximal plane graph, with n vertices and three special vertices a_1, a_2, a_3 in clockwise order around the outer face.

3-orientation

Definition 7.1. An orientation of the inner edges of T is a *3-orientation* if every inner vertex has outdegree three. From the count of edges it follows that the special vertices a_i are sinks in every 3-orientation.

Schnyder wood

Definition 7.2. An orientation and coloring of the inner edges of T with colors red, green and blue is a *Schnyder wood* if:

(1) All edges incident to a_1 are red, all edges incident to a_2 are green and all edges incident to a_3 are blue.

(2) Every inner vertex v has three outgoing edges colored red, green and blue in clockwise order. All the incoming edges in an interval between two outgoing edges are colored with the third color, see Figure 19.

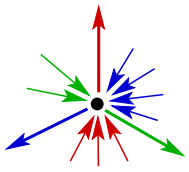

Figure 19: Schnyder's edge coloring rule.

Theorem 7.1. *Let T be a plane triangulation with outer vertices a_1, a_2, a_3. Schnyder woods and 3-orientations of T are in bijection.*

The proof is very similar to the proof of Theorem 2.1. Given an edge e which is incoming at v, we can classify the outgoing edges at v as left, straight and right. Define the straight-path of an edge as the path which always takes the straight outgoing edge. A count and Euler's formula shows that every straight-path ends in a special vertex. The special vertex where a straight-path ends determines the color of all the edges along the path. It can also be shown that two straight-paths starting at a vertex do not rejoin. This implies that the coloring of the orientation is a Schnyder wood.

From this proof it follows that the local properties (1) and (2) of Schnyder woods imply:

(3) *The edges of each color form a tree rooted at a special vertex and spanning all the inner vertices.*

Recall that in the case of separating decompositions we also found the tree decomposition being implied by local conditions (c.f. item (3) after the proof of Theorem 2.1).

Note.

Schnyder woods were introduced by Schnyder in [37] and [38]. They have numerous applications in the context of graph drawing, e.g., [4, 8, 32], dimension theory for orders, graphs and polytopes, e.g., [37, 9, 21], enumeration and encoding of planar structures, e.g., [34, 24]. The connection with 3-orientations was found by de Fraysseix and Ossona de Mendez [14].

The aim of this section is to prove the following theorem of Bonichon.

Theorem 7.2. *The total number of Schnyder woods on triangulations with $n+3$ vertices is*

$$V_n = C_{n+2}\, C_n - C_{n+1}^2 = \frac{6\,(2n)!\;(2n+2)!}{n!\;(n+1)!\;(n+2)!\;(n+3)!}$$

where C_n is the Catalan number.

Before going into details we outline the proof. We first show a bijection between Schnyder woods and a special class of bipolar orientations of plane graphs. We trace these bipolar orientations through the bijection with separating decompositions, twin pairs of trees and triples of non-intersecting paths. Two of the three paths turn out to be equal and the remaining pair is a non-crossing pair of Dyck paths. This implies the formula.

Note.

The original proof, Bonichon [7], and a more recent simplified version, Bernardi and Bonichon [6], are also based on a bijection between Schnyder woods and pairs of non-crossing Dyck paths. In [6] the authors also enumerate special classes of Schnyder woods.

Little is known about the number of Schnyder woods of a fixed triangulation. In [22] it is shown that the maximal number of Schnyder woods a triangulation on n vertices can have is asymptotically between $2,37^n$ and $3,56^n$. As with 2-orientations, the computational complexity of the counting problem is unkown.

Proposition 7.1. There is a bijection between Schnyder woods on triangulations with $n+3$ vertices and bipolar orientations of maps with $n+2$ vertices and the special property:

($\star$) The right side of every bounded face is of length two.

Proof. Let T be a triangulation with a Schnyder wood S. With (T, S) we associate a pair (M, B), where M is a subgraph of T and B a bipolar orientation on M. The construction is in two steps. First we delete the edges of the green tree in S and the special vertex of that tree, i.e., a_2, as well as the two outer edges incident to a_2, from the graph, the resulting graph is M. Then we revert the orientation of all blue edges and orient the edge $\{a_3, a_1\}$ from a_3 to a_1, this is the orientation B. Figure 20 shows an example.

The orientation B has a_3 as unique source and a_1 as unique sink. To show that it is bipolar we verify properties V and F. Property V requires that at a vertex $v \neq s, t$ the edges partition into nonempty intervals of incoming and outgoing edges, this is immediate from the edge coloring rule (2) and the construction of B.

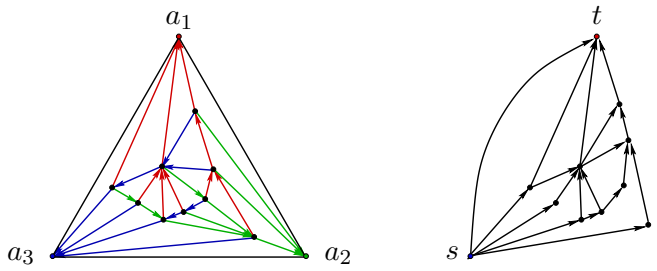

Figure 20: A Schnyder wood and the corresponding bipolar orientation.

For Property F consider a bounded face f of M. Suppose that f is of degree > 3, then there had been some green edges triangulating the interior of f. The coloring rule for the vertices on the boundary of f implies that these green edges form a fan, as indicated in Figure 21. From the green edges we recover, again with the coloring rule, the orientation of the boundary edges of f in B: the neighbors of the tip vertex of the green edges are the unique source and sink of f. This also implies that the right side of f is of length two, i.e., $(\star)$.

If f is a triangle, then two of its edges are of the same color, say red. The coloring rule implies that these two edges point to their common vertex, whence the triangle has unique source and sink. Since the transitive vertex of f has a green outgoing edge in S, it is on the right side and $(\star)$ also holds for f.

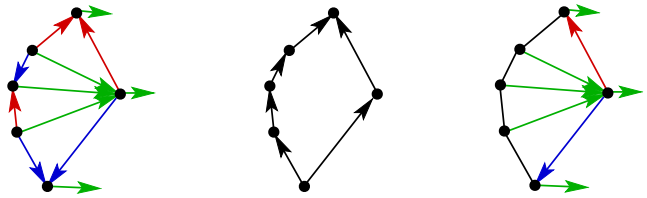

Figure 21: From a generic face in S to B and back.

For the converse mapping, consider a pair (M, B) such that $(\star)$ holds. Every vertex $v \neq s, t$ has a unique face where it belongs to the right side. This allows us to identify the red and the blue outgoing edges of v. Property $(\star)$ warrants that there is no conflict. The green edges are the edges triangulating faces of larger degree together with edges reaching from the right border to the additional outer vertex a_2. This yields a unique Schnyder wood on a triangulation. □

Given a plane bipolar orientation (M, B) with $n + 2$ vertices and the $(\star)$ property, we apply the bijection from Proposition 5.3 to obtain a quadrangulation Q with a separating decomposition. Property $(\star)$ is equivalent to

$(\star')$ Every white vertex (except the rightmost one) has a unique incoming edge in the blue tree.

In particular it follows that there is a matching between vertices $v \neq s, t$ and bounded faces of M, hence, in Q there are $n + 2$ black and $n + 1$ white vertices.

The separating decomposition of Q yields twin-alternating trees with $n + 1$ black and n white vertices (Theorem 2.2). From the twin-alternating pair we get to a twin binary pair of trees with $n + 1$ black and n white vertices (Theorem 4.1). This pair of trees yields a

triple of non-intersecting paths (Theorem 4.3). Figure 22 shows an example of the sequence of transformations.

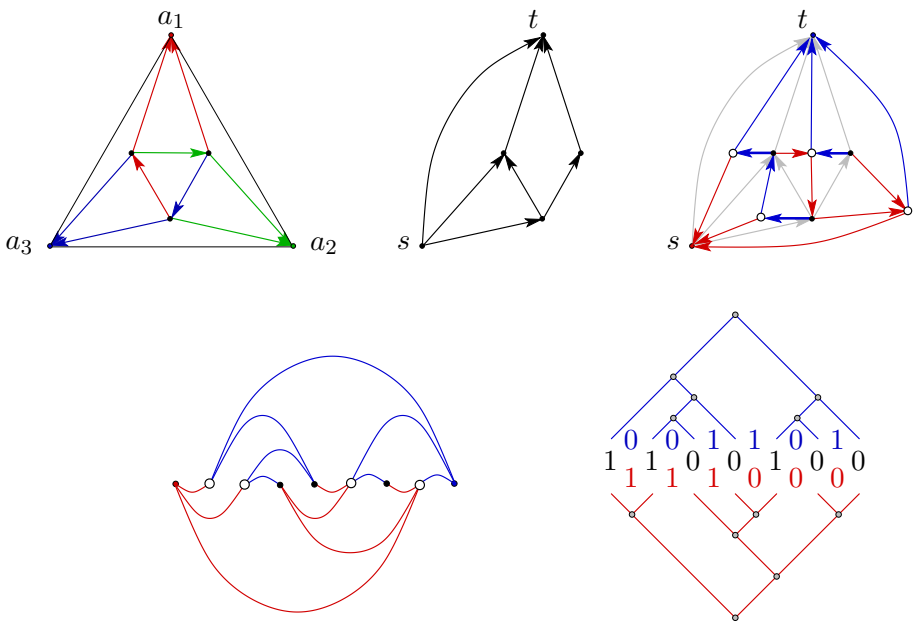

Figure 22: From a Schnyder wood to three strings.

From $(\star')$ we get some crucial properties of the fingerprint and the bodyprints of the blue tree T^b and the red tree T^r.

Fact 1. If we add a leading 1 to the reduced fingerprint $\hat{\alpha}$, then we obtain a Dyck word; in symbols $(01)^n \leq_{\mathsf{dom}} 1 + \hat{\alpha}$.

Proof. It is better to think of $1 + \hat{\alpha}$ as the fingerprint α^b of the blue tree after removal of the last 0. Property $(\star')$ implies that there is a matching between all 1's and all but the last 0's in the α^b, such that each 1 is matched to a 0 further to the right. △

Fact 2. The fingerprint uniquely determines the bodyprint of the blue tree, precisely $\overline{\beta^b} = 1 + \hat{\alpha}$.

Proof. From $(\star')$ it follows that $\alpha^b_i = 1$ implies $\beta^b_{i+1} = 0$. Since α^b has n entries 1 and β^b that same number of 0's, it follows that β^b is determined by α^b. △

Let $\alpha^* = 1 + \hat{\alpha}$ and $\beta^* = 1 + \hat{\beta}^r$; then $(01)^n \leq_{\mathsf{dom}} \alpha^* \leq_{\mathsf{dom}} \beta^*$. We omit the proof that actually every pair (α^*, β^*) of 0,1 strings from $\binom{2n}{n}$ with these properties comes from a unique Schnyder wood on a triangulation with $n+3$ vertices. Translating the resulting bijection with strings into the language of paths we obtain:

Theorem 7.3. *There is a bijection between Schnyder woods on triangulations with $n+3$ vertices and pairs (P_1, P_2) of non-intersecting upright lattice paths, where P_1 is from $(0,0)$ to (n,n), P_2 is from $(1,-1)$ to $(n+1, n-1)$, and the paths stay weakly below the diagonal, i.e., they avoid all points (x,y) with $y > x$.*

For the actual counting of Schnyder woods we again apply the lemma of Gessel and Viennot. The entry $A_{i,j}$ in the matrix is the number of paths from the start of P_i to the end of P_j staying weakly below the diagonal. The reflection principle of D. André allows us to write these numbers as differences of binomials.

Proposition 7.2. The number of Schnyder woods on triangulations with $n+3$ vertices is

$$\det \begin{pmatrix} \binom{2n}{n} - \binom{2n}{n-1} & \binom{2n}{n+1} - \binom{2n}{n-2} \\ \binom{2n}{n-1} - \binom{2n}{n-2} & \binom{2n}{n} - \binom{2n}{n-3} \end{pmatrix} = \frac{6\,(2n)!\,(2n+2)!}{n!\,(n+1)!\,(n+2)!\,(n+3)!}$$

Acknowledgements. Mireille Bousquet-Mélou and Nicolas Bonichon are greatly thanked for fruitful discussions.

References

[1] E. Ackerman, G. Barequet, and R. Pinter, *On the number of rectangulations of a planar point set*, J. Combin. Theory Ser. A, 113 (2006), pp. 1072–1091.

[2] M. Aigner, *A Course in Enumeration*, vol. 238 of Graduate Texts in Mathematics, Springer-Verlag, 2007.

[3] J. D. Annan, *The complexity of the coefficients of the Tutte polynomial*, Discr. Appl. Math., 57 (1995), pp. 93–103.

[4] I. Bárány and G. Rote, *Strictly convex drawings of planar graphs*, Documenta Math., 11 (2006), pp. 369–391.

[5] R. J. Baxter, *Dichromatic polynomials and Potts models summed over rooted maps*, Annals of Combinatorics, 5 (2001), p. 17.

[6] O. Bernardi and N. Bonichon, *Catalan intervals and realizers of triangulations*. `arXiv.org:0704.3731`.

[7] N. Bonichon, *A bijection between realizers of maximal plane graphs and pairs of non-crossing Dyck paths*, Discrete Mathematics, 298 (2005), pp. 104–114.

[8] N. Bonichon, S. Felsner, and M. Mosbah, *Convex drawings of 3-connected planar graphs*, Algorithmica, 47 (2007), pp. 399–420.

[9] G. Brightwell and W. T. Trotter, *The order dimension of convex polytopes*, SIAM J. Discrete Math., 6 (1993), pp. 230–245.

[10] T. Brylawski and J. Oxley, *The Tutte polynomial and its applications*, in Matroid Applications, Cambr. Univ. Press, 1992, pp. 123–225.

[11] N. Chiba, T. Nishizeki, S. Abe, and T. Ozawa, *A linear algorithm for embedding planar graphs using PQ-trees*, J. Comput. Syst. Sci., 30(1) (1985), pp. 54–76.

[12] F. Chung, R. Graham, V. Hoggatt, and M. Kleiman, *The number of Baxter permutations*, J. Comb. Theory, Ser. A, 24 (1978), pp. 382–394.

[13] R. Cori, S. Dulucq, and G. Viennot, *Shuffles of pharentesis systems and Baxter permutations*, J. Comb. Theory, Ser. A, 43 (1986), pp. 1–22.

[14] H. de Fraysseix and P. O. de Mendez, *On topological aspects of orientation*, Discr. Math., 229 (2001), pp. 57–72.

[15] H. de Fraysseix, P. O. de Mendez, and J. Pach, *A left-first search algorithm for planar graphs*, Discrete Computational Geometry, 13 (1995), pp. 459–468.

[16] H. de Fraysseix, P. Ossona de Mendez, and P. Rosenstiehl, *Bipolar orientations revisited*, Discrete Appl. Math., 56 (1995), pp. 157–179.

[17] P. O. de Mendez, *Orientations bipolaires*, PhD thesis, École des Hautes Études en Sciences Sociales, Paris, 1994.

[18] S. Dulucq and O. Guibert, *Stack words, standard tableaux and Baxter permutations*, Discr. Math., 157 (1996), pp. 91–106.

[19] S. Dulucq and O. Guibert, *Baxter permutations*, Discr. Math., 180 (1998), pp. 143–156.

[20] S. Felsner, C. Huemer, S. Kappes, and D. Orden, *Binary labelings for plane quadrangulations and their relatives*. `arXiv:math.CO/0612021`, 2007.

[21] S. Felsner and S. Kappes, *Orthogonal surfaces*, Order, (2008). DOI:10.1007/s11083-007-9075-z.

[22] S. Felsner and F. Zickfeld, *On the number of planar orientations with prescribed degrees.* arXiv:math.CO/0701771.

[23] E. Fusy, *Straight-line drawing of quadrangulations*, in Proceedings of Graph Drawing '06, vol. 4372 of LNCS, 2007, pp. 234–239.

[24] E. Fusy, D. Poulalhon, and G.Schaeffer, *Dissection and trees, with applications to optimal mesh encoding and random sampling*, in Proc. 16th ACM-SIAM Symp. Discr. Algo., 2005, pp. 690 – 699.

[25] E. Fusy, D. Poulalhon, and G. Schaeffer, *Bijective counting of bipolar orientations*, Electr. Notes in Discr. Math., (2007), pp. 283–287.

[26] I. Gelfand, M. Graev, and A. Postnikov, *Combinatorics of hypergeometric functions associated with positive roots*, in The Arnold-Gelfand Mathematical Seminars: Geometry and Singularity Theory, V. I. e. a. Arnold, ed., Birkhäuser, 1997, pp. 205–221.

[27] I. Gessel and G. Viennot, *Binomial determinants, paths, and hook length formulae*, Adv. Math., 58 (1985), pp. 300–321.

[28] O. Guibert and S. Linusson, *Doubly alternating Baxter permutations are Catalan*, Discr. Math., 217 (2000), pp. 157–166.

[29] I. B.-H. Hartman, I. Newman, and R. Ziv, *On grid intersection graphs*, Discr. Math., 87 (1991), pp. 41–52.

[30] G. Kant and X. He, *Regular edge labeling of 4-connected plane graphs and its applications in graph drawing problems*, Theor. Comput. Sci., 172 (1997), pp. 175–193.

[31] A. Lempel, S. Even, and I. Cederbaum, *An algorithm for planarity testing of graphs*, in Theory of Graphs, Int. Symp (New York), 1967, pp. 215–232.

[32] C. Lin, H. Lu, and I.-F. Sun, *Improved compact visibility representation of planar graphs via Schnyder's realizer*, SIAM J. Discrete Math., 18 (2004), pp. 19–29.

[33] C. Mallows, *Baxter permutations rise again*, J. Comb. Theory, Ser. A, 27 (1979), pp. 394–396.

[34] D. Poulalhon and G. Schaeffer, *Optimal coding and sampling of triangulations*, in Proceedings ICALP '03, vol. 2719 of Lecture Notes Comput. Sci., Springer-Verlag, 2003, pp. 1080–1094.

[35] P. Rosenstiehl and R. E. Tarjan, *Rectilinear planar layouts and bipolar orientations of planar graphs*, Discrete Comput. Geom., 1(4) (1986), pp. 343–353.

[36] G. Rote, I. Streinu, and F. Santos, *Expansive motions and the polytope of pointed pseudo-triangulations*, in Discrete and Computational Geometry, The Goodman and Pollack Festschrift, vol. 25 of Algorithms and Combinatorics, Springer, 2003, pp. 699–736.

[37] W. Schnyder, *Planar graphs and poset dimension*, Order, 5 (1989), pp. 323–343.

[38] W. Schnyder, *Embedding planar graphs on the grid*, in Proc. 1st ACM-SIAM Symp. Discr. Algo., 1990, pp. 138–148.

[39] N. J. A. Sloane, *The on-line encyclopedia of integer sequences*. `http://www.research.att.com/~njas/sequences`.

[40] R. P. Stanley, *Enumerative Combinatorics*, vol. 2, Cambridge Univ. Press, 1999.

[41] R. Tamassia and I. G. Tollis, *A unified approach to visibility representations of planar graphs*, Discrete Comput. Geom., 1(4) (1986), pp. 321–341.

[42] R. Tamassia and I. G. Tollis, *Planar grid embedding in linear time*, IEEE Trans. on Circuits and Systems, CAS-36(9) (1989), pp. 1230–1234.

[43] M. Yannakakis, *Embedding planar graphs in four pages*, J. Comput. System Sci., 38 (1986), pp. 36–67.